







This is to certify that the

thesis entitled

AN ANALYTICAL METHOD FOR PREDICTION OF CHATTER STABILITY IN A BORING OPERATION

presented by

Mukund Rajamony Iyer

has been accepted towards fulfillment of the requirements for

MS Mechanical Engineering
degree in

Date 5/12/00

MSU is an Affirmative Action/Equal Opportunity Institution

0-7639

PLACE IN RETURN BOX to remove this checkout from your record. TO AVOID FINES return on or before date due. MAY BE RECALLED with earlier due date if requested.

DATE DUE	DATE DUE	DATE DUE

11/00 c/CIRC/DateDue.p65-p.14

AN ANALYTICAL METHOD FOR PREDICTION OF CHATTER STABILITY IN A BORING OPERATION

Ву

Mukund Rajamony Iyer

A THESIS

Submitted to

Michigan State University

in partial fulfillment of the requirements

for the Degree of

MASTER OF SCIENCE

Department of Mechanical Engineering

2000

Abstract

AN ANALYTICAL METHOD FOR PREDICTION OF CHATTER STABILITY IN A BORING OPERATION

By

Mukund Rajamony Iyer

An analytical method for the prediction of chatter stability in boring is developed. The dynamics of the boring process is obtained by combining a mechanistic cutting force model with the structural dynamics of the boring bar. Chip regeneration in the axial direction has been given importance in the dynamics of the process. Friction is not taken into account and the system is assumed to be linear. The chatter stability analysis is based on a delay-differential equation model. The solution of the first order characteristic system of this equation is used to compute the chatter stability lobes of the machining process. This model can be used to quickly compute the chatter stability of a multi-insert boring operation. The results obtained from this method are compared with time domain simulations and experiments.

To my family

Acknowledgements

I would like to express my deepest appreciation to the following people for having made the completion of this thesis possible:

To my advisor Dr. Brian Feeny, for his guidance and invaluable assistance, without which this thesis would not have been possible.

To my other committee members, Dr. Steve W. Shaw and Dr. Dinesh Balagangadhar, for their valuable suggestions and comments.

To Dr. Suresh Jayaram, Process Simulation and Analysis Tools Division, Caterpillar Inc., with whom this idea was formulated during the summer of 1999. His dedications to the subject and personal integrity have served as an example and an inspiration to me.

To Dr. Robert Ivester and Dr. Matt Davies, NIST, for the help provided in setting up the experiment collecting data. Also to Dr. Tony Schmitz and Dr. Jon Pratt, for the fruitful discussions we had at NIST.

To all my other instructors at MSU, for their skillful instruction in the classroom, but more importantly, for their friendship and constant encouragement.

To my friends, 'Marcus', 'Vetti', 'Bill' and 'Tiger', for having made my stay at MSU a memorable experience.

To my family, for years of support, patience and understanding.

And to GOD, for all the blessings showered upon me.

Table of Contents

Lis	st of tables		vii
Lis	st of figures		viii
Ke	y to Symbols	or Abbreviations	ix
1.	Introduction		
	1.	1 Machining of Metals	1
	1.	2 Machine Tool Vibrations	3
	1.	3 High Speed Machining	4
2.	Literature Su	rvey and Problem Description	
	2.	1 General Machining Operations	7
	2.	2 Boring	12
	2.	3 Problem Description	15
3.	Theory		
	3.	1 Introduction	18
	3.	2 Cutting Force Model	23
	3.		20
	3.	4 Formulation	28
		3.4.1 Single Insert Boring: N=1	29
		3.4.2 Twin Insert Boring: N=2	30
	3.	5 Time Domain Simulations	33
	3.	6 Delay Differential Equations	34
	3.		37
4.	Results and I	Discussion	
	4.	1 Measurements and Simulation	39
		4.1.1 Single Insert Boring	4(
		4.1.2 Two Insert Boring	41
	4.	2 Measurements done at NIST	43
		4.2.1 Short boring Bar	45
		4.2.2 Long boring Bar	54
	4.	3 Discussion	60
5.	Conclusions		63
6.	Suggestions	for future work	64

Bibliography			66
Appendix			
	Α	Fig. 28 Section Y-Z of a single insert boring operation	70

List of Tables

1.	Structural dynamics of the cutter	40
2.	Calibration Constants	44
3.	Modal parameters of the Short bar	48
4.	Cutting Coefficients	52
5.	Modal parameters of the Long bar	57

List of Figures

1.	A stability chart for a boring operation	6
2.	Schematic of a boring operation	18
3.	Single insert work piece interaction	20
4.	Cutting Forces for Twin Insert Boring Bar at 4500 rpm and 0.75 mm	
	Depth of Cut	35
5.	Cutting Forces for Twin Insert Boring Bar at 4500 rpm and 0.85 mm	
	Depth of Cut	35
6.	Experimentally Measured Frequency response figures for the boring bar	40
7.	Stability Chart for a Single-insert Boring	41
8.	Stability Chart for a Two-insert Boring	42
9.	Experimental set up	45
10.	Magnitude of Transfer function G _{xx} (s)	46
11.	Magnitude of Transfer function G _{yy} (s)	47
12.	Magnitude of Transfer Function G _{zz} (s)	47
13.	Axial accelerations for stable depth of cut 0.381 mm	49
14.	Axial accelerations for unstable depth of cut 1.016 mm	49
15.	FFT analysis for the 1st second of stable cut operation	50
16.	FFT analysis for the 5 th second of stable cut operation	51
17.	FFT analysis for the 1st second of unstable cut operation	51
18.	FFT analysis for the 5 th second of unstable cut operation	52
19.	Stability Lobes for the short boring bar	53
20.	Chatter Signature of the short boring bar	54
21.	Magnitude of Transfer function G _{xx} (s)	55
22.	Magnitude of Transfer function G _{yy} (s)	56
23.	Magnitude of Transfer function Gzz(s)	56
24.	Stability Lobes for the Long boring Bar	57
25.	Chatter Signature of the Long Boring Bar	58
26.	FFT analysis for the 3 rd second of a stable cut operation	59
27.	FFT analysis for the 3 rd second of an unstable cut operation	59
28.	Section Y-Z of a single insert boring operation	57

Key to Symbols or Abbreviations

SYMBOL	MEANING	UNITS
F _a	Axial Cutting Force	N
$\mathbf{F}_{\mathbf{r}}$	Radial Cutting Force	N
$\mathbf{F_t}$	Tangential Cutting Force	N
G_{ij}	Displacement Transfer function in i-direction due to force in the j	m/N
	direction	
K _a	Axial Cutting force coefficient	N/m2
K _r	Radial Cutting force coefficient	N/m2
K _t	Tangential Cutting force coefficient	N/m2
N	Number of inserts	
T	Time period at a point between successive inserts	s
$\mathbf{d}_{\mathbf{d}}$	Depth of cut	m
$\mathbf{f_d}$	Dynamic feed	m
f_s	Static feed	m
Rpm	Revolutions per minute of the cutter	revs/min
Δz	Chip regeneration in axial direction	m
Δr	Chip regeneration in radial direction	m
фі	Insert angle with respect to y-axis	rad
ϕ_{inc}	Angle between successive inserts	rad
ϕ_1	Lead angle of the insert	rad
ω	Chatter frequency	rad/s

Chapter 1: Introduction

Section 1.1: Machining of Metals

Machining of metals has been studied extensively over the last hundred years, the focus primarily being on reduction of machining costs and a pragmatic approach to the manufacture of parts of acceptable dimensional accuracy and surface quality. Metal cutting phenomena were visualised and published as early as 1945 by Merchant [1]. Three important reasons define the necessity to develop a predictive theory for the metal cutting process [2]:

- A predictive metal cutting theory would be beneficial to process planners by providing sufficient knowledge of process efficiency.
- A predictive metal cutting theory would be beneficial to the tool designers, producers,
 and users, as it constitutes a proper basis for making right decisions.

A predictive metal cutting theory would benefit designers and users of machine tools
by providing them with real process parameters such as cutting forces, heat
generation rate and energy consumption.

Boring, drilling, facing, milling, reaming and turning constitute the machine tool operations widely used in industry. Boring, drilling and reaming are generally the processes for producing internal cylindrical surfaces, i.e., holes of moderate accuracy in terms of position, roundness and straightness. These processes are typically done on engine lathes or milling machines, in addition to specialized tools on a transfer line. Drilled holes are often used for mechanical fasteners like bolts or rivets. Drilling a hole is a preliminary step for processes like tapping, boring or reaming. Internal cylinders of moderate accuracy are produced by drilling and high accuracy internal cylinders are produced by boring, in both cases the feed motion is axial. Turning and facing are lathe processes which involve using a single cutting edge with specified geometry in constant contact with workpiece to remove material. Relative motion is achieved by rotating the workpiece. Due to this relative motion, the tool either moves parallel or normal to the axis of rotation making lathes the best at producing surfaces of revolution. The sides of an external cylinder are produced by turning when the feed motion is parallel to the axis of rotation. The ends of a cylinder are generated by facing, where the feed motion is radial and normal to the axis of rotation. Milling machines are extremely productive as they employ multiple cutting edges as opposed to single cutting edges. The cutting speed is generated by rotating the cutter and moving the workpiece in a plane normal to the axis of spindle rotation. Milling processes are used to produce contour and planar surfaces.

Common types of milling are face and end milling [3].

Section 1.2: Machine Tool Vibrations

Due to inherent stiffness and damping properties of a tool and workpiece, vibrations during the cutting process are a common occurrence. Machine tool vibrations have been widely studied and a lot of progress has been made in order to suppress unwanted vibrations occurring during the operation. Machine tool vibrations are a very important problem in the manufacturing industry. Undesired vibration may lead to problems, viz., poor surface finish, tool wear and noise on the shop floor resulting in a loss of productivity. An operation displaying any or all of the symptoms above is said to chatter.

Chatter is a nuisance to metal cutting and its effects are adverse. Chatter effects surface finish, dimensional accuracy, tool wear and machine life. Surface finish undulations are generally defined as chatter marks. Velocity variations on the tools due to imbalance in the drive system, servo instability or stick slip friction, can result in periodical variations in the surface finish.

However, forced vibrations and self-excited vibrations are the major sources of chatter. Forced vibrations can be attenuated by reducing the driving force and/or the dynamic compliance to permissible values.

Many theories have been propounded to analyze self-excited chatter.

Advancements in machining speed and machining of thermal alloys have resulted in the want of a better understanding of self-excited chatter [4].

Section 1.3: High Speed Machining

The speed range of a machining process is measured by the DN number. DN is defined as the product of the diameter in mm and the spindle speed in rpm. DN is closely related to the surface cutting speed which is of the form

$$v = \pi D N, \tag{1}$$

where

D= is the cutter diameter, (m)

N= is the rotational speed of the spindle, (revs/sec)

Smith and Tlusty [5] showed that for a tool of diameter 25mm and dominant natural frequency 1000Hz, low range machining speed extends upto 2300 rpm, mid range between 2300 and 7500 rpm and high range extends beyond 7500 rpm. The upper limit of mid range machining is where the tooth passing frequency is $1/4^{th}$ of the natural frequency.

There have been many instances in machine tool operations where large quantities of material had to be removed, especially in milling. Advances in tool materials have made it possible to reduce time by high-speed milling. Generally, high-speed machining

ranges between spindle speeds of 7,500 and 50,000 rpm for the same tool described above. High speed machining leads to the employment of large axial and radial depths of cut paving the way for dramatic improvements in metal removal rates [6].

Mid range machining varies from speeds of 2300 rpm to 7500 rpm. It was shown that mid range machining did not have any process damping effects as in low speed machining [5]. Process damping will be discussed later. A stability chart shows the maximum depth of cut or feed a machining operation can undergo without chatter for a given spindle rpm. A typical stability chart is shown in Fig.1. The stability lobes shown here mark the boundary between stable and unstable cuts of operation, the area below the lobes representing stable operation zones and the area above, unstable operating zones. It can be seen from the figure that there are many stability lobes in the given range of speed and, given sufficient power, the operation can be suitably tuned to machine larger depths of cut or feed, thereby making the process more and more efficient. Tlusty and Zaton [7] showed that the mid-range asymptotic stability limit was fairly constant and the machine operation could be improved by spindle speed variation and non-proportional tooth spacing. Our focus, in this work, lies on mid range and high speed machining.

In high speed machining, the stable depth of cut depends very strongly on the spindle speed. It also displays a constant stability limit as in mid-range machining. It has been observed that increases in metal removal rates can be obtained if the tooth passing frequency is a fraction of the most dominant natural frequency.

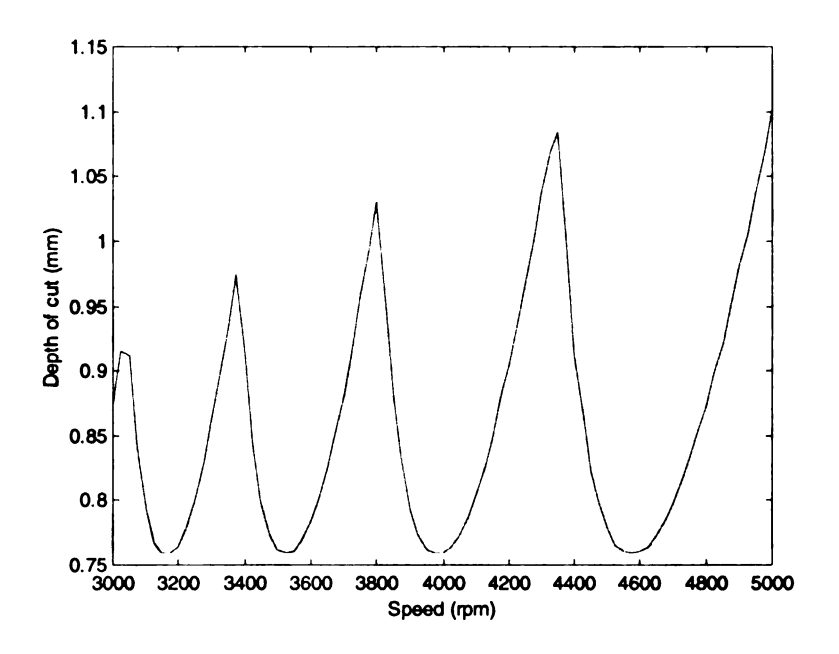


Fig. 1 A stability chart for a boring operation.

The goal of the work done here is to develop an analysis tool to generate stability lobes for a boring operation quickly and reliably. A detailed statement of the problem is given in the following chapter.

Chapter 2: Literature Survey and

Problem Description

Section 2.1: General Machining Operations

Early attempts were made to examine the effect of flexible supports on the modes of vibration of a machine tool [8]. The goal of the analyses was to determine whether these supports would isolate a vibration without causing the machine tool to chatter. The force due the action of the tool on the workpiece was found to be a function of the vibration amplitude and tool speed among other factors. When chatter occurs, this force was such that the inherent damping of one of the modes was overcome and an oscillation was sustained at a frequency not far from the resonance frequency of the modes. The machine tool structure was assumed to be a collection of spring-mass systems, each having a specific resonance frequency. Findings showed that the chatter frequency was one of the frequencies whose peak was least damped. It was also shown that the tool wear

primarily depended on the chatter velocity. From their studies, it was concluded that direct use of isolators would not help in vibration isolation and chatter simultaneously if the frequencies causing chatter were low.

Following this, a theory was developed to compute the stability lobes of a machine tool system [4]. However, this theory excluded the dynamics of the cutting process. Chatter was reasoned out to be caused primarily by the dynamic stiffness of the system. Merritt also claimed that chatter would be a minor problem if the damping ratios of the most affecting modes was of the order of ξ =0.5. Merritt also suggested that this theory, developed for the turning process, could easily be extended towards other processes.

A model [9] was proposed for metal cutting analysis on a milling machine. The model comprised of simple linear differential coefficients with perodic coefficients. The model also took into consideration the rotation of induced forces. The equations were of first order and were very convenient for stability analysis. A regeneration factor, μ , was introduced. The instantaneous chip thickness was now the sum of the nominal feed and the total deviation in the chip thickness. The deviation is computed from the vibration of the workpiece and the surface generated at that point due to the passage of the previous tooth. From the model, it was concluded that chatter analysis was associated with the stability characteristics of linear differential equations with periodic coefficients. Sridhar also concluded that stability methods, based on frequency analysis, could not be used to study chatter in milling operations.

Sridhar et al. [10] followed up with their previous theory and came up with a stability algorithm for the general milling process. The algorithm involved the solution of a transcendental equation by employing existing graphical solution methods. Sridhar used a linear theory, which, in the past, was found to sufficiently accurate. The algorithm presented an elegant technique for solving for more realistic models.

Tlusty and Zaton [7] used a time domain simulation approach to develop a better understanding of milling stability. Many previous assumptions, such as uniform orientation of all the cutter teeth, were abolished. The theory showed that the gains in stability were actually smaller than they were previously thought to be. However, time domain simulations are very tedious and take a long time to predict a stability chart.

Smith and Tlusty [6] showed that the optimum speed of operating a milling operation would be in the region of its natural frequency since the regeneration of waviness on the surface, which causes chatter stability, inhibited the development of forced vibrations. Subsequent work by Smith and Tlusty [11] resulted in the development of a control system to adjust the spindle speed and the feed rate automatically to achieve stable milling. Other algorithms employed to study stability were Peak to Peak Diagrams of forces, deflections or surface finishes [12].

A new method for the prediction of chatter in milling was propounded by Minis and Yanushevsky [13]. The dynamics of the milling process were described by a set of

differential equations with time varying periodic coefficients and time delays. The resulting characteristic equation was of infinite order and its truncated version was used to determine the limit of stability by employing standard techniques of control theory. Excellent agreement with previous experimental results was the validity of the proposed stability method.

Based on transfer functions of the structure of the cutter workpiece contact zone, and the static force coefficients, a new analytic method was presented to predict the stability lobes in the milling operation by Altintas and Budak [14]. This analysis showed that frequency domain simulations could be performed on the milling operations. The method was shown to yield the stability diagram much faster, and of the same accuracy or better, compared to conventional time domain methods, used in the past. The method was based on the formulation of dynamic milling with regeneration in the chip thickness. The theory was robust and was able to incorporate time varying modal parameters into its algorithm.

Tlusty [15] suggested that in the case of high speed machining operations, tool dynamics could be effectively manipulated to get the best out of the spindle. Chatter was also found due to the varying flexibility of the workpiece during machining.

High speed machining became a very economically significant process. Smith and Tlusty [5] discussed how attempts to make practical use of high speed machining led to developments in tool materials, spindle and machine design, chatter avoidance and

structural dynamics of machine tools to name a few.

Chen, Ulsoy and Koren [16] presented a computational stability analysis for turning. The solution scheme was simple since the characteristic equation simplified to the solution of a single variable. It was also suggested that this method could be employed for other machining processes, as long as the system equations were expressed as a set of linear time-invariant difference differential equations.

Rao and Shin [17] presented a model of the dynamic cutting force process for the three-dimensional or oblique turning operation. The methodology involved linking the mechanistic force model to the tool-workpiece vibration model. Cross coupling between radial and axial states was paid particular attention to as this inclusion was believed to be important in predicting the unstable-stable chatter phenomenon occurring due to non-linearity in the process.

More recently, Bayly, Halley and Young [18] came up with a quasi-static model for reaming. This model neglected inertial and damping forces, but included regeneration and rubbing effects. The eigenvalue solution was found to closely resemble the tool behavior seen in practice. The same authors also came up with another simulation of radial chatter in drilling and reaming [19].

Section 2.2: Boring

Boring bars are metal cutting tools that are used to bore deep precise holes in a variety of manufacturing operations. These cutting holes are used after a hole has already been made from a drilling operation. The boring bar is characterized by a large length-to-diameter (L/D) ratio. The boring bar is clamped at one end by a tool holder, and has a cutting insert at the free end. The cutting insert at the free end is used to cut the metal in the bore of the workpiece to a close tolerance. The cutting operation is achieved either by keeping the boring bar stationary and moving the workpiece or vice versa.

A boring bar is characterized by a low transverse dynamic stiffness. Hence, it is susceptible to excessive mechanical vibrations in the transverse direction. Merritt [4] had earlier shown metal cutting processes, including boring, as a closed loop feedback system. This system can be explained from the fact that the motion of the tool in the previous tool pass affects the force acting on the cutting tool in its current pass.

Until recently, most of the machine tool operations were developed for milling and turning, as discussed before, and suitably modified for boring. Few theories were built specifically for the boring process.

One early study by Anshoff [20] was in the field of chatter suppression. Anshoff concluded that there were two ways to suppress chatter. One was to fit an absorber on the

boring head. The second method was to utilize certain bar materials of high damping capacity such as manganese copper.

Chatter free machining was reported if the longitudinal flats were machined on the bar and a suitable position was selected for the cutting tool in the boring head. The depth of the cut was analyzed to be sensitive to changes in the angle of the tool with respect to the plane of the flats (lead angle) [21].

Parker [22] showed that boring could be well modeled if the penetration rate effect (or the dependence of the forces on the velocity of the tool) was considered. The force due to this effect was proportional to the process damping constant. However, recent research has revealed that process damping, talked about previously, assumes an important role only in low speed machining and has very little or no effect in mid-range and high speed machining. Parker concluded that tangential vibrations were an important consideration at certain head angles as their exclusion caused serious problems to the simulation.

Rivin [23] suggested a structural optimization approach to improve the dynamic stability of the boring bars with long overhangs. Little effort was made to simulate stability charts of boring operations.

Kapoor et al. [24] developed an elegant mathematical model based on dynamic equations in which chip regeneration was an important parameter. The model involved

development of a transfer function, which made it not only possible for predicting boring bar chatter but also predicting the generation of irregularities on the surface. The formulation eliminated chip regeneration from the feedback path in the closed loop system, thereby greatly simplifying the simulation. Zhang and Kapoor [25] followed this method with particular attention to tangential vibrations. The simulations yielded good results with some discrepancies in the stability lobes.

Tewani et al. [26] suggested the boring bar to be extremely susceptible to chatter owing to its cantilever type structure which reduced its dynamic stiffness in the transverse directions. He suggested that chatter free boring bars are typically of the overhang ratio 4.5 and less.

Recently, Li, Ulsoy and Endres [27] showed that there exist differences between stationary and rotating bores. The work was primarily focussed on regenerative chatter due to tool rotation. Stability lobes varied for stationary and rotating bores. Qualitative explanations were given without mathematical proof to show the discrepancies between exact and approximate solutions, especially at low spindle speeds.

The regeneration term (the increment or decrement in material removal rate due to the difference between the current and previous insert depths) affects the stability limit. The proposed analysis is for high speed and mid range machining. Since the feed rate is much slower than the speed range of the boring process, full chip regeneration in the axial direction of the boring bar is assumed, i.e, μ =1.

Several analytical methods have been used in the past to compute the stability limits [4, 13, 28]. It is possible to linearize the non-linear cutting force model and use the linear model to compute the chatter stability limits. However, these linear models are only accurate close to the region of linearization and will introduce errors if extrapolated over wide ranges [27, 29]. The assumption of no nose radius implies that the analytical results can be applied to tools where the depth of cut is significantly larger than the nose radius. Analytical models which include the effect of nose radius and depth of cut variations have been overcome in recent work by Ozdoganlar et al. [28]. These methods can be incorporated into the present analytical method to make the model more comprehensive. The analytical model proposed in this work provides a quick means to estimate the stability limits. Emphasis is laid on vibrations in the feed or the axial direction. If a detailed analysis is required, then the more accurate time domain simulation can be performed.

Section 2.3: Problem Description

This work aims to develop a simple analytic method for the prediction of chatter limits in a boring operation. The eigen-value method developed by Altintas [14] for milling has been extended towards the boring operation. The boring bar is assumed to be stationary while the workpiece rotates. Certain assumptions have been made in view of previous experiences in analysing similar machine tool operations.

- Properties in the X, Y and Z directions have been considered and incorporated into the
 equations. Though the tool is considered stiffer in the axial directions, properties have
 been included as they have an effect on the analysis. Torsion effects have been
 neglected.
- The cutting forces are assumed to be linearly dependent on the depth of cut and the feed, thereby linearly proportional to the chip area.
- Cutting coefficients are treated to be constant for the range of spindle speed
 considered. The spindle speed we are concerned with is between 3,000 and 15,000
 rpm. Hence, coefficients related to penetration rate and velocity variation have been
 removed to make the analysis simple.
- The structure is assumed to be linearly and proportionally damped.
- The tool lead angle has been taken into account, but no nose radius has been used.
 However the theory can be easily extended to incorporate nose radius changes.
- The inserts are spaced at equal angles and the inserts are equally distant from the center of the boring bar.
- Extreme cases of boring resulting in no contact between tool and workpiece have been neglected in the simulation.

The work is organized as follows: The Theory section describes the method of analysis. Following the theory are the results obtained using the formulation developed in this work. The formulation is compared with a time domain simulation. Models are also verified with experimental results. Application of the theory is discussed in the

Discussion part. A brief summary follows the discussion. Scope for possible future work is also discussed at the end.

Chapter 3: Theory

Section 3.1: Introduction

A boring bar as described previously, is a tool with a large length-to-diameter (L/D) ratio. L/D ratios vary typically from 2 to 9. A simple diagram of a boring bar is shown in Fig. 2.

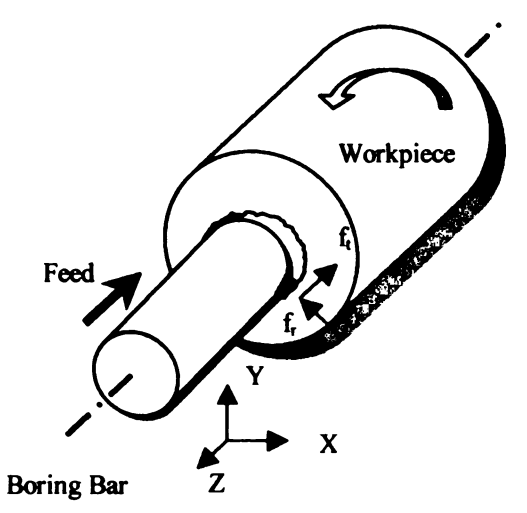


Fig. 2 Schematic of a boring operation

The above figure is a model of a 2 insert boring bar. The boring bar is assumed to be irrotational and feeding in the negative Z direction. For the insert shown, f_r and f_t are the radial and tangential forces experienced by the tool during the cutting process. In addition to this, the tool also experiences an axial force f_{ax} in the positive Z-direction. The radial and tangential forces, shown in fig. 2, are on the X-Y plane. The workpiece is assumed to rotate in the problem of our concern.

If the bar is assumed as a perfectly uniform beam free at the loaded end and clamped at the other, the static stiffness for the bending motion is given by

$$K_s = \frac{3EI}{L^3},\tag{1}$$

where,

E= modulus of elasticity, N/m²

I= transverse moment of inertia in the x direction, m⁴, and

L= length of the beam, m

Clearly from Eq.1, it is evident that the longer the boring bar, the more weaker it is in the transverse directions. This weakness in transverse stiffness is a primary cause for chatter.

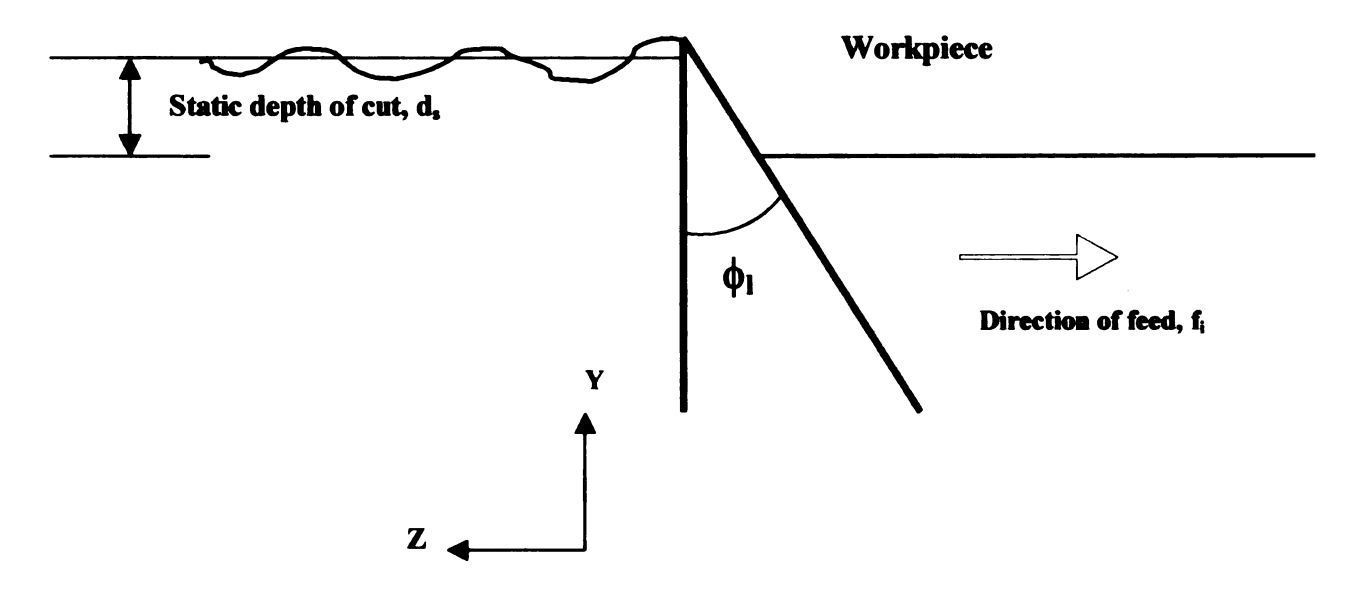


Fig. 3 Single insert workpiece interaction

The movement of the boring bar in the negative Z-direction is called the feed as shown in Fig. 3. A detailed diagram of a Y-Z section of a single insert boring operation is shown in the Appendix A. Feed is typically expressed in mm/rev or mm/sec. The instantaneous feed rate is obtained as the sum of the static feed rate, the projection of the current vibration in the direction of the feed, and the projection of the previous vibration (imprinted on the workpiece surface) in the direction of the feed. The static feed rate, f_s is defined as the feed rate with which the operation begins. Hence, the instantaneous feed for the i^{th} -cutting insert can be represented by the following equation:

$$f_i = f_{ri} + \Delta z + \Delta r \tan(\phi_i), \tag{2}$$

where,

$$\Delta r = x \sin(\phi_i) + y \cos(\phi_i) - x_o \sin(\phi_i - \phi_{inc}) - y_o \sin(\phi_i - \phi_{inc}), \tag{3}$$

and,

$$\Delta z = z - \mu z_{\alpha} \tag{4}$$

x, y, and z are the deflections of the cutter at time t and x_0 , y_0 , and z_0 are the deflections of the cutter at time t-T, i.e., one revolution before. T defines the period of revolution of the workpiece, the inverse of which multiplied by 60, gives the workpiece rpm. At the time t-T, the workpiece was at an angle ϕ_t - ϕ_{inc} to the Y-axis. It must be noted that the angle, ϕ_t , is the angle of the current insert with respect to the Y-axis and the angle, ϕ_t - ϕ_{inc} , is that of the previous cutting insert. This is different from the turning and milling operations where the angle, ϕ_t , is used for both [14].

Since there exists a possibility of the tool overlapping part of the surface previously cut, a regeneration parameter, μ is introduced in Eq.4. In the case of spiral cutting as observed in a threading process, the previous tool position has no relation to the present position. Hence μ is assumed to be 0. The feed of the system is slow as compared to the machining speed concerned in our analysis. Owing to this, a large portion of the tool tip machines the same surface in the axial direction for a number of revolutions of the workpiece. Therefore, the regeneration factor μ is assumed as 1. The

regeneration direction of the boring bar is in the axial direction since the tool is moving in the Z-direction.

The radial position of the tool tip with respect to the workpiece in the radial direction is defined as the instantaneous depth of cut. For this analysis, the depth of cut is a parameter to be found. When looking at linear stability, we consider either (a) purely linear systems or, (b) small deviations from equilibrium, which would not involve the machine tool leaving the cut. Hence, the extreme case where the tool insert exits cut, i.e., the tool does not touch the surface of the workpiece (a clear case of chatter) has been left out. Time domain analysis can be used to predict exactly and speeds and the feed where the tool inserts exits cut. This phenomenon is regarded as tool run out. The instantaneous depth of the cut for the i^{th} insert is represented by d_i . A boring process typically moves in the feed direction, hence, the dynamics are assumed to be primarily in the feed direction. Dynamics in the depth of cut direction have been omitted since our main focus of interest lies in the axial direction, which is also the feed direction. Fig. 3 shows a typical case of tool dynamics indicating a static depth of cut, the direction of feed and the lead angle.

Eq. (2) also shows the effect of lead angle on the feed. The vibrations in the X and Y directions affect the feed in the Z-axis [30]. The lead angle is defined as the angle made by the tool as shown in Fig. 3. Lead angles are typically from -20 to +20 degrees for boring bars [31]. The lead angle is shown in Fig.3.

Section 3.2: Cutting Force Model

We assume that each insert i is oriented at angle ϕ_i to the Y axis. The inserts on the tool are spaced equally apart. The forces on a single insert is given by

$$\begin{cases}
f_t \\
f_r \\
f_{ax}
\end{cases} = \begin{cases}
K_t \\
K_r \\
K_{ax}
\end{cases} A_c$$
(5)

Eq. 5 takes into account only the dynamic chip area. The dynamic chip area is defined as below:

$$A_c = f_i d_i - f_{ij} d_i \tag{6}$$

The dynamic chip area for the ith insert is defined as the difference between the instantaneous chip area and the static chip area. The static chip area does not influence the dynamics of the system and therefore is removed from the analysis. The static chip area does not result in tool chatter. The depth of cut is a parameter to be found.

 K_t , K_r and K_{ax} are cutting coefficients in the tangential, radial and axial directions respectively. Cutting coefficients are found by running experiments in the static cutting region and evaluating forces that occur in the tangential, radial and axial directions. The forces are then divided by the chip area of the cutting process to obtain cutting coefficients. Hence the involvement of the static feed occurs only the evaluation of the

cutting coefficients. This evaluation of the cutting coefficients is valid only in the stable zone of operation, where vibrations to the tool are damped out and stabilized. Cutting forces are approximated as linear functions of static feed and the static depth of cut only for mid-range and high speed machining processes. For low speed machining processes, the forces are not a true linear function of the feed and the depth of cut. Therefore, prediction of cutting coefficients is difficult to make. This analysis assumes linearized cutting coefficients. More on cutting coefficients is discussed in section 3.7.

Using Eqs. 2, 3, 4 and 6 into Eq. 5, we obtain

$$\begin{cases}
f_{t} \\
f_{r} \\
f_{ax}
\end{cases} = \begin{cases}
K_{t}d \tan(\phi_{t}) & K_{t}d \\
K_{r}d \tan(\phi_{t}) & K_{r}d \\
K_{ax}d \tan(\phi_{t}) & K_{ax}d
\end{cases} \begin{bmatrix} \Delta r \\ \Delta z \end{bmatrix}$$

$$(7)$$

The matrix C contains the cutting coefficients. The forces experienced by each tool insert can be conveniently transformed in the global X, Y and Z directions by the following expression:

$$\begin{cases}
F_x \\
F_y \\
F_z
\end{cases}_i = \begin{bmatrix}
-\cos(\theta_i) & -\sin(\theta_i) & 0 \\
\sin(\theta_i) & -\cos(\theta_i) & 0 \\
0 & 0 & -1
\end{bmatrix} \begin{cases}
f_i \\
f_r \\
f_{ax}
\end{cases}_i$$
(8)

Tr, in the above equation is the transformation matrix. In order to compute the chatter stability limits, it is assumed that the system is vibrating at the chatter frequency, ω The chatter frequency is simulated over a range of frequencies. Altintas [14] used a frequency range of ½ the lowest modal frequency to 2 times the highest modal frequency of the tool in his analysis. It was argued in his analysis that the chatter frequency is found in the range of the modal frequencies of the tool of operation. Our analysis intends to do the same. The system is also assumed to be harmonic, i.e., the deflections at the cutter at time t-T are obtained by multiplying $e^{-i\omega T}$ to the deflections at the cutter at time t. T is defined as the tooth passing period, the inverse of which is called the tooth passing frequency. This frequency is also equal to the rps of the workpiece multiplied by the number of inserts or teeth, N on the tool. Writing in matrix form we have,

This expression represents synchronous periodic motion. Later we will find conditions that allow for periodic motion. This will represent the transition between stable (exponentially decaying) and unstable (exponentially growing) regimes. Eq. 7, along with Eqs. 3 and 4, shows the dependence of the axial, radial and tangential forces on an insert tip to be dependent on the X, Y and Z vibrations of the boring bar at time t and the x, y, z vibrations of the insert at a previous time t-T. The x, y, z vibrations of the insert are the same as the surface undulation on the workpiece. The term $i\omega$ is represented also by the Laplace transform variable s.

Eqs. 3 and 4 can be rewritten into a single matrix equation using Eq. 10 as:

$$\begin{cases}
\Delta \mathbf{r} \\
\Delta z
\end{cases} = \begin{bmatrix}
\sin(\theta_i) - e^{-i\omega I} \sin(\theta_i - \theta_{inc}) & \cos(\theta_i) - e^{-i\omega I} \cos(\theta_i - \theta_{inc}) & 0 \\
0 & 0 & 1 - e^{-i\omega I}
\end{bmatrix} \begin{bmatrix} \mathbf{x} \\ \mathbf{y} \\ z \end{bmatrix} \tag{10}$$

Note the restriction of periodic motion is incorporated into P.

Section 3.3: Structural Dynamics Model

The vibrations in the X, Y and Z directions can be computed from the forces by using the transfer function matrix. In the Laplace transfer frequency domain, the expression governing this relation is given by:

$$\begin{cases}
x(s) \\
y(s) \\
z(s)
\end{cases} = \begin{bmatrix}
G_{xx}(s) & G_{xy}(s) & G_{xz}(s) \\
G_{yx}(s) & G_{yy}(s) & G_{yz}(s) \\
G_{xx}(s) & G_{zy}(s) & G_{zz}(s)
\end{bmatrix} \begin{bmatrix}
F_{x}(s) \\
F_{y}(s) \\
F_{z}(s)
\end{bmatrix} \tag{11}$$

The forces $F_x(s)$, $F_y(s)$ and $F_z(s)$ represent the Laplace transform of the forces exerted on the cutting tool due to the interaction of all the inserts with the workpiece. In

mathematical terms, the forces in the time domain are computed by summing up the individual forces exerted on each insert as shown below in Eq. 12.

$$\begin{cases}
F_x \\
F_y \\
F_z
\end{cases} = \sum_{i=1}^{N} \begin{cases}
F_x \\
F_y \\
F_z
\end{cases} \tag{12}$$

Eq. 11 has a transfer function matrix G(s). Element $G_{ij}(s)$ is the transfer function between the deflection in the i^{th} direction due to the force in the j^{th} direction. There could be a possibility of more than one mode existing in a particular direction influenced by a force in another direction. Merritt [4] showed the importance of using transfer functions in machining operations. Element $G_{ij}(s)$ can be written mathematically as

$$G_{ij}(s) = \sum_{n=1}^{number of \bmod es} \left(\frac{1/m_n}{s^2 + 2\xi_n \omega_n(s) + \omega_n^2} \right), \tag{13}$$

The mass (m_n) , damping ratio (ξ_n) and frequency (ω_n) are the n^{th} modal parameters of the dominant modes in the i^{th} direction influenced by the force in the j^{th} direction. Elements G_{xx} , G_{yy} and G_{zz} are known as the direct transfer functions. The rest are known as cross transfer functions.

It has been observed that direct transfer functions are more influential in the transfer function matrix and the cross transfer functions are smaller in magnitude compared to the direct transfer functions. Hence, for simplicity, the cross transfer

functions are eliminated. Eq. 11 is rewritten as

Section 3.4 Formulation

Eqs. 7, 8, 10 and 12 are combined in Eq. 14 to give

$$\begin{cases} x \\ y \\ z \end{cases} = [G] \sum_{i=1}^{N} [Tr] C [P] \begin{cases} x \\ y \\ z \end{cases}$$
 (15)

The problem has two parameters, the depth of cut d and the tooth-passing period T. The preceding formulation is restricted to synchronous harmonic motion. Matrix P incorporates this restriction. Indeed, such a response representing the transition between stable and unstable cutting can occur under specific circumstances, for which Eq. 15 has a non-trivial solution. We can determine these circumstances by solving for d and T. The non-trivial solution to Eq. 15 is possible if the determinant

$$I - \left[G\right] \sum_{i=1}^{N} \left[Tr \left[C\right]P\right] = 0$$
 (16)

Eq. 16 is a characteristic equation used to solve for two variables, T and d. The fact that d, the depth of cut, is a real number is made use of in finding the solution for T, by setting the imaginary parts of d to zero.

Section 3.4.1: Single Insert Boring: N=1

We assume the insert to be aligned along the Y-axis, i.e., θ_1 =0°. Also since there is only one insert, θ_{inc} =360°. Each element of Eq. 16, Tr, C, P and G can be determined separately and put back into Eq.16 yielding the characteristic equation

$$1 + K_{ar}d(1 - e^{-i\omega T})G_{rr} + K_{r}d\tan(\phi_{r})G_{rr}(1 - e^{-i\omega T}) = 0$$
 (17)

Eq. 17 does not involve $G_{xx}(s)$, i.e., the transfer function in the X-direction related to the Force in the X-directon. It was earlier assumed that the insert was located on the Y-axis. $G_{xx}(s)$ plays a role in Eq. 17 if the insert is located on the X-axis. Substituting

$$\Lambda = 1 - e^{-i\omega T} \tag{18}$$

into Eq.17, the depth of cut can be solved as

$$d = \frac{1}{2} \cdot \frac{1}{\text{Re}(K_{ax}G_{zz} + K_{r} \tan(\phi_{l})G_{w})}$$
 (19)

and T can be solved from the expression,

$$Cot\left(\frac{\omega T}{2}\right) = 2d\operatorname{Im}(K_{ax}.G_{z} + K_{r} \tan(\phi_{l})G_{yy})$$
 (20)

The spindle speed is then obtained by using the expression

$$\Omega = \frac{60}{NT},\tag{21}$$

N being equal to 1 in this case.

Section 3.4.2: Twin insert boring, N=2

In the case of twin insert boring, Eq. 16 involves a summation of the interaction between both the inserts. The inserts are placed such that $\theta_1=0^{\circ}$, $\theta_2=180^{\circ}$ and $\theta_{inc}=180^{\circ}$. Eq. 16 is simplified to obtain a determinant,

$$\begin{vmatrix} 1 & 2K_{t}d \tan(\phi_{t})G_{yy}(1+e^{-i\omega t}) & 0\\ 0 & 1+2K_{r}d \tan(\phi_{t})G_{yy}(1+e^{-i\omega t}) & 0\\ 0 & 0 & 1+2K_{ax}dG_{zz}(1-e^{-i\omega t}) \end{vmatrix} = 0,$$
 (22)

Once again, $G_{xx}(s)$ is absent because the inserts are aligned along the Y-axis. The analysis therefore shows that transfer function in the X-direction do not have an effect on

the solution of our system. However, it is also observed that the modal parameters in the x and y directions are very similar and therefore, will affect the solution in a similar way. Two solutions arise from the solution of the determinant shown in Eq. 22. The first solution is solely dependent on the axial cutting coefficient and the axial modal parameters. The second solution involves the lead angle ϕ_i and modal parameters in the y direction. Each of these solutions for the depth of cut d have a corresponding spindle speed Ω . The lowest depth of cut corresponding to a speed is considered for the stability plot.

Solution 1: Eqn. 22 is satisfied if

$$1 + 2K_r d \tan(\phi_t) G_{vv} (1 + e^{-i\omega t}) = 0$$
 (23)

Eq. 23 can be solved, bearing in mind that d can only be real. The solution for d would then be

$$d = \frac{1}{\tan(\phi_l)} \left[-\frac{1}{4 \cdot \text{Re}(G_{yy})} \right], \tag{24}$$

and the solution of T can be obtained from,

$$\tan\left(\frac{\omega T}{2}\right) = 2d\operatorname{Im}(-2K_{r}d\tan(\phi_{t})G_{yy})$$
 (25)

The spindle speed can be computed from the time T by employing Eq. 21.

Solution 2: Eqn. 22 is also satisfied if

$$1 + 2K_{ax}dG_{z}(1 - e^{-i\omega t}) = 0 (26)$$

from which, the solution for d is,

$$d = -\frac{1}{4.K_{ax}.\operatorname{Re}(G_z)},\tag{27}$$

and T can be obtained by solving,

$$\cot\left(\frac{\omega T}{2}\right) = 2d\operatorname{Im}(2K_{ax}G_{z}) \tag{28}$$

Again, the spindle speed, Ω , is derived from T using Eq. 22. The data obtained from Eqs. 26 thru 29 are charted and the lowest positive depth of cut for a particular spindle speed is selected as a stability limit.

Eqs. 19 and 27 show the strong dependence of the axial parameters on the depth of cut. The dependence of the stability boundaries on axial parameters is the main thrust of this work

Multi-insert solutions can also be obtained from the analytic method. However experimental data for chatter stability of multi insert boring bars is yet to be found to validate the theory.

Section 3.5: Time Domain Simulations

Simulation of machining operations for a certain number of revolutions at a given range of speeds and depths of cut is known as time domain simulations. Time domain simulations are very accurate. However, these simulations must be performed for each value of depth of cut and speed. Hence, the time taken to plot a stability chart is large. Analytic methods are preferred to time domain simulations when time is a constraint. The time domain simulation algorithm is a general algorithm that can also be used for boring processes. In operations such as milling, facing and turning, there are entry and exit angles, i.e., angles where the insert enters and exits cut every time the tool bar rotates. In the case of boring, the insert is always removing material and actually does not enter and exit the cut at any time. Extreme cases of insert run-out due to excessive vibration have been neglected, as these cases are a sure example of chatter.

The time step or the angular increment of the tool rotation depends on the speed of operation. Jayaram, 1997 [32] showed that the angular increment should satisfy the inequality $\pi/(\omega_n*10) \geq 60*\theta_{inc}/(\Omega*360)$. This means, $\theta_{inc} \leq \Omega*6/(20*f_n)$. The smallest angular increment required for $\Omega=1000$ rpm and $f_n=500$ Hz is 0.6°. Hence, a value of 0.5° was used for these simulations.

The algorithm was used to work on 10 passes or 10 revolutions of the workpiece over the tool. Therefore, for example, an operation for 5000 rpm was simulated for 2 ms.

Forces in the X, Y and Z directions were plotted for the simulated time and the system was said to chatter if the forces were observed to grow. This phenomenon of growth in forces could be readily observed in a single insert boring bar. In a multi insert boring bar, due to the symmetry of the forces in the simulation, the resultant forces acting on the structure is minimal, causing no excitation of the structure. This phenomenon could be observed in the force plot of a time domain simulation as shown in Figs. 4 and 5. An artificial spike is introduced which simulates a hard spot or a poor workpiece material at a particular place. Then the force plot is observed after the introduction of the spike. If this spike causes the vibrations to increase with time (become unstable) then this condition is termed as chatter. The depth of cut was incremented in steps of 0.05 mm until chatter was detected. The criterion for the detection of chatter is to determine if any of the cutting forces, f_x , f_y or f_z , or the dynamic feed rate increases with time after the first few revolutions.

Section 3.6: Delay Differential Equations

Let us examine a simple case of a single insert boring. The insert is at angle $\theta=0^{\circ}$ with respect to the Y-axis. The forces then acting on the insert are

$$\begin{cases}
f_{t} \\
f_{r} \\
f_{ax}
\end{cases} = \begin{cases}
K_{t}d_{s} \tan(\phi_{t}) & K_{t}d_{s} \\
K_{r}d_{s} \tan(\phi_{t}) & K_{r}d_{s} \\
K_{ax}d_{s} \tan(\phi_{t}) & K_{ax}d_{s}
\end{cases} \begin{bmatrix}
y - y_{o} \\
z - z_{o}
\end{bmatrix},$$
(29)

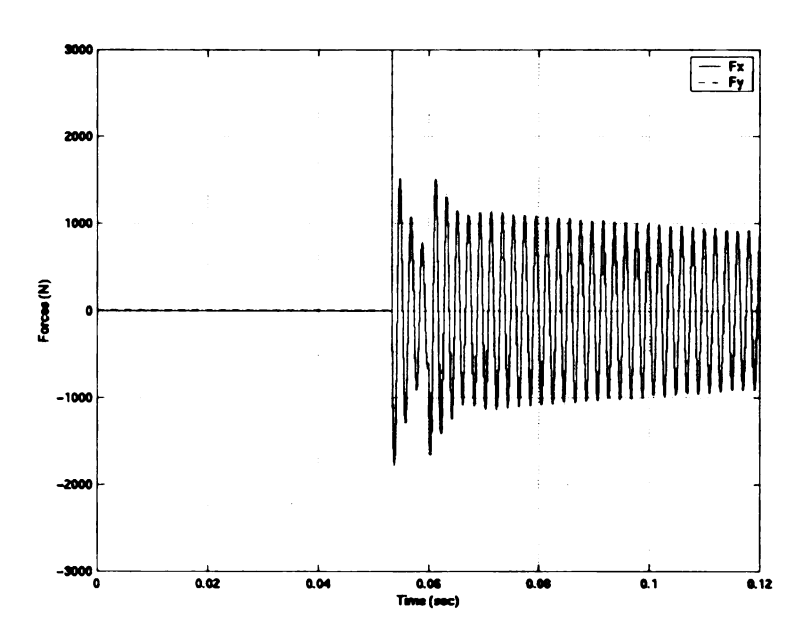


Fig. 4 Cutting Forces for Twin Insert Boring Bar at 4500 rpm and 0.75 mm Depth of Cut.

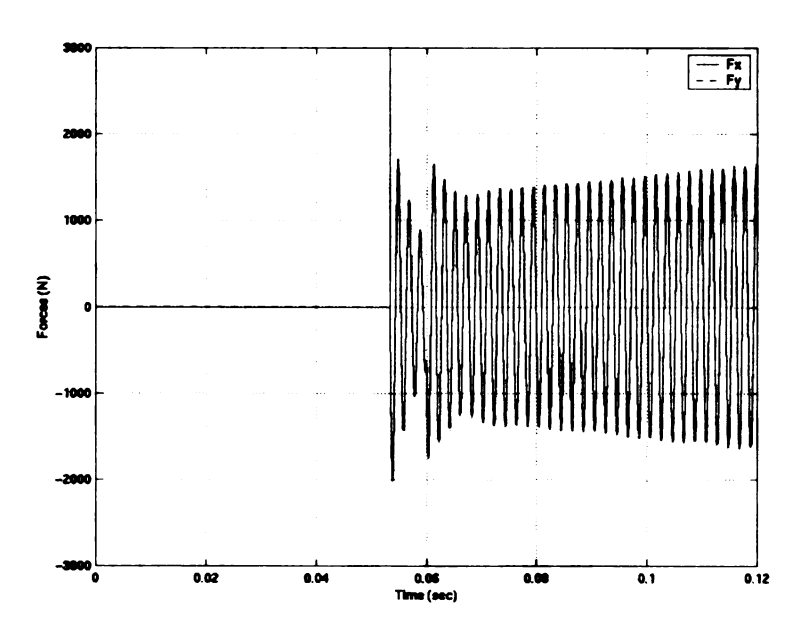


Fig. 5 Cutting Forces for Twin Insert Boring Bar at 4500 rpm and 0.85 mm Depth of Cut.

The forces in the radial, tangential and axial directins can be transformed to the global X,Y and Z coordinates. With the aid of the modal parameters of the tool obtained from impact hammer tests, the forces in the X,Y and Z directions can be used to compute the dynamics of the tool. Therefore,

$$\begin{cases}
F_x \\
F_y \\
F_z
\end{cases} = \begin{cases}
m_x x + c_x x + k_x x \\
m_y y + c_y y + k_y y \\
m_z z + c_z z + k_z z
\end{cases} = \begin{cases}
-f_t \\
-f_r \\
-f_{ax}
\end{cases}$$
(30)

Eqs. 29 and 30 indicate that the forces are delay differential equations. These equations contain delay in two parameters, y and z, and a single time delay of T. A delay differential equation is one in which the derivative of a parameter x at a time t can be expressed as a function of x (and its lower order derivatives) at time t and at earlier instants [33]. Delay differential equations appear in many fields such as physics & engineering, biology, medicine and economics.

Let us consider a problem of the type

$$y'(t) + ay(t) + by(t - \omega) = f(t), t \in [0, \infty)$$

$$y(t) = \phi(t), t \in [-\omega, 0]$$
(31)

The first observation in trying to solve the above set of equations is to reduce it to a sequence of ode's.

$$y'(t) + ay(t) = f(t) - b\phi(t - \omega), t \in [0, \omega]$$

$$y(0) = \phi(0)$$
(32)

This method is then continued onto $[\omega, 2\omega]$, $[2\omega, 3\omega]$ and so on. In this way, an approximate solution is achieved on a finite set $\{t_1, ..., t_n\}$ with $0 \le t_1 \le ... \le t_n \le \omega$ (together with values for the derivatives from eq. 33). Using these values, an approximate solution on the whole interval $[0,\omega]$ is created by Hermite Interpolation with piecewise polynomials [34].

Section 3.7: Estimation of Cutting Coefficients

Shaw [35] has worked on methods to estimate the cutting forces, thereby evaluate the cutting coefficients. The forces are established in terms of the specific energy (u) since this remain the same for a given work material. The cutting force in the direction of the feed is assumed to approximately be equal to one half of the tangential force. The radial force is typically neglected in the evaluation presented by Shaw.

The specific energy varies approximately with the undeformed feed as

$$u \approx \frac{1}{f^{0.2}} \tag{33}$$

The value of the cutting coefficient is approximately the value of the specific energy of the system. Shaw has discussed elaborately showing the variation of the cutting forces with complex chip formation and variations in cutting speeds.

Chapter 4: Results and Discussion

Section 4.1: Measurements and Simulation

A single-insert and a twin-insert boring bar are used to validate the chatter stability limits. A solid-carbide boring bar is used to remove stock from a hardened steel material (AISI51200 with Rc=57). The feed rate used for the cutting tests was 0.2032 mm/tooth and the lead angle on the tool was 2°. The linearized cutting coefficients in the radial, tangential and axial directions were experimentally determined to be K_r=5.5915e5 N/m², K_r=5.4745e5 N/m², and K_a= 2.4382e5 N/m² from static cutting tests. The boring bar modal parameters were experimentally obtained using impact hammer tests. The measured frequency response functions (FRF's) are shown in Figure 6 and the estimated dominant modal parameters are shown in Table 1.

Table 1: Structural Dynamics of the cutter

	ω _n (Hz)	K(N/m)	ξ
X	494.1	2.94e8	0.055
Y	472.6	2.64e8	0.056
Z	495.9	3.06e9	0.049

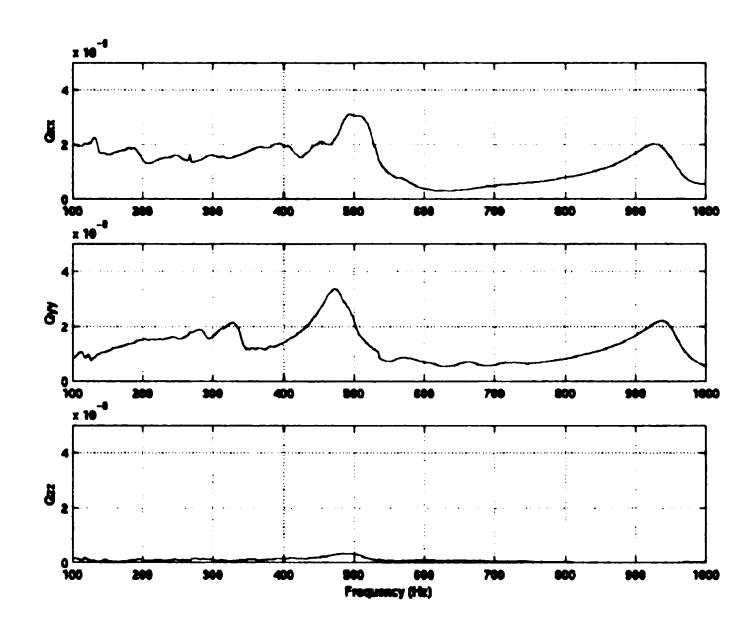


Fig. 6 Experimentally measured Frequency response figures for the boring bar

Section 4.1.1: Single Insert Boring

The comparison of the analytical method and time domain solutions are shown in Figure 7. From this figure, it can be seen that the difference between the asymptotic depth of cut obtained using the time domain and the analytical method is less than 5%. The

time domain solution is computed using a numerical Runge-Kutta solution technique.

It has been observed that cutting coefficients are fairly similar for mid-range machining. Low speed machining involves cutting coefficients that are functions of speed and depth. This analytic prediction is useful for machining processes where the speed reduces changes in cutting coefficients. Hence, certain discrepancies in the time domain and analytic predictions were observed.

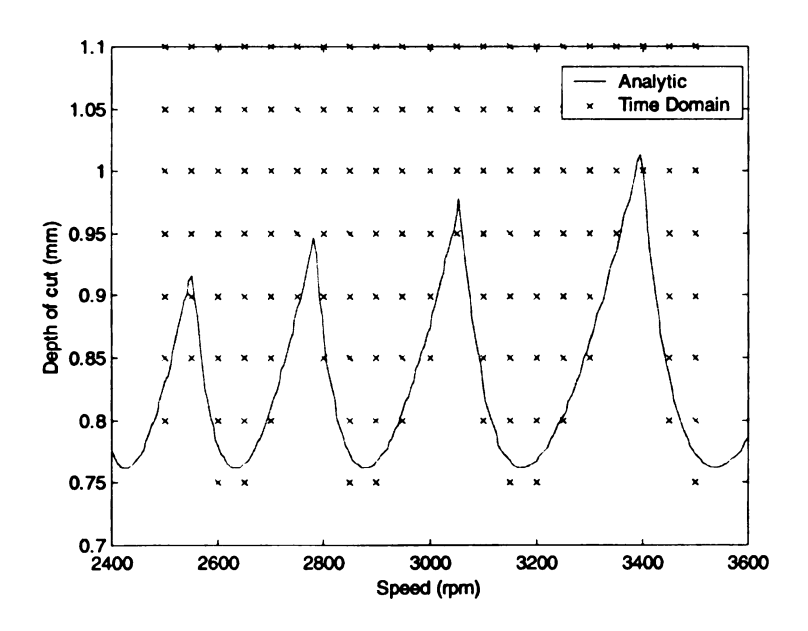


Fig. 7 Stability chart for a single-insert boring operation.

Section 4.1.2: Two Insert Boring Operation

The same modal parameters were taken for a two insert bore and the stability

tables calculated analytically was compared with the numerical time domain simulations in Fig. 8. It was observed that the analytic simulation was able to capture the limits very well.

Both figures 7 and 8 show a comparison between the results obtained from analytical and time domain methods. With these stability lobes, a boring operation could be altered suitably in terms of speed and depth of cut to move from an unstable region to a stable region. Depths such as 0.7 mm in Fig.6 which is unstable at speeds close to 4100 rpm, could be increased to as high as 1.5 mm at 5000 rpm to achieve a stable depth of cut and therefore increase the productivity. For e.g. if a boring operation required 3 passes at 0.7 mm depth of cut and 4500 rpm, it would require 2 passes if the speed were slightly increased to 5000 rpm. However, this assumes that the machine operating the boring bar has sufficient power to provide a speed range where the stability lobes play a crucial role.

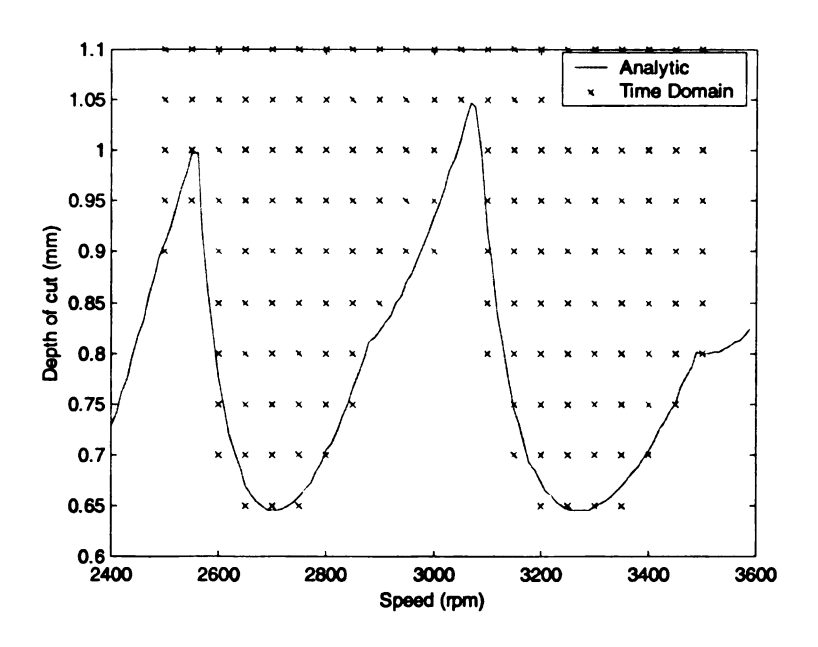


Fig. 8 Stability chart for a two-insert boring operation.

The modal parameters and cutting coefficients were used to predict the consistency of time domain simulations with the frequency domain analytic technique used here. Ideally, there should be no deviation between the time domain simulation performed and the analytic method used. One source of error could be the time integration step in the time domain simulation. Another source of possible error could also lie in the analytic method which is based on the assumption that synchronous harmonic motion occurs at the transition between stable and unstable cuts of operation. No experimental tests were performed for the single and two insert boring bars.

Section 4.2: Measurements Done at NIST

An experiment was conducted at NIST to measure the depth of cut and the chatter frequency of operation. Fig. 9 shows the experimental setup. The experimental setup shows the operation of machining material from the outside of the circular workpiece rather than the inside of the workpiece, which is a typical boring operation. The time domain and frequency domain analyses can be used for this kind of operation. The workpiece material was mild steel of the type AISI 10-45. Two single insert boring bars were analysed. One was a short boring bar with an overhang of 110 mm from the face holder and the other was a long bar with an overhang of 127 mm from the face holder. An impact hammer test was performed for each of the tools to obtain the frequency response functions. Based on the impact hammer tests, the acceleration transfer functions were recorded. The hammer and accelerometer signals were amplified through a PCB

model 482A17 4-channel amplifier and recorded using a Hewlett-Packard 35670A dynamic signal analyser. A Kemo dual Variable Filter 10 m anti-aliasing filter of 2.5kHz was used to prevent aliasing of higher frequencies. The calibration chart is provided in Table 2. The Impact Hammer was a PCB 086C04.

The acceleration transfer functions were measured for a bandwidth of 6.4 kHz with a frequency resolution of 4 Hz. From the transfer functions recorded, a matlab script frf_plot.m (Courtesy: Tony Schmitz, NIST) was used to plot the transfer function magnitudes of the tool in the X, Y and Z directions.

Table 2: Calibration Constants

INSTRUMENT	CALIBRATION	UNITS
Accelerometer SN 21208	9.684e-4	V/m/s ²
Impact Hammer SN 9775	1.240e-3	V/N

In order to prevent the chip from interfering with the accelerometers and causing damage to them, the accelerometers were placed as close to the edge as possible.

Cutting tests were performed and acceleration time responses of the cutting action of the tools were recorded on an oscilloscope. Time domain samples of the responses in the three directions were recorded using a sampling time interval of 50 μ s. The number of samples was as large as 115,000 so as to collect time responses for as long as 6.75 s.

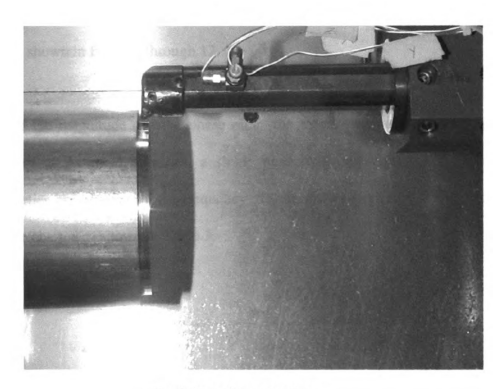


Fig. 9 Experimental setup

Section 4.2.1: Short boring Bar (110 mm overhang from the face holder)

In the first case, a single insert boring operation with a short boring bar of overhang 110 mm from the face holder was taken. The insert was a CCMT 3252-F2 TP 30 type carbide insert with a TiN coating to improve wear resistance and tool life. The accelerometer was placed on the boring bar as close as possible to the insert. Assuming the boring bar to behave like a cantilever beam with an overhang, the accelerations in the X, Y and Z directions were increased by 10% to account for the postitioning of the accelerometers as shown in fig. 9. To reduce the effect of the nose radius, the cutting tests were conducted with a depth of cut more than the nose radius. From the analysis of the transfer functions, it was seen that the cross transfer functions have a very low magnitude as compared with the direct transfer functions. The magnitudes of the direct transfer

functions are shown in Figs. 10 through 12.

Using the magnitude and the phase plots, the modal parameters of the tool are evaluated. For all practical purposes, a single peak frequency and its corresponding modal properties are observed for a frequency. The modal properties in the X, Y and Z directions are charted as shown in Table 3.

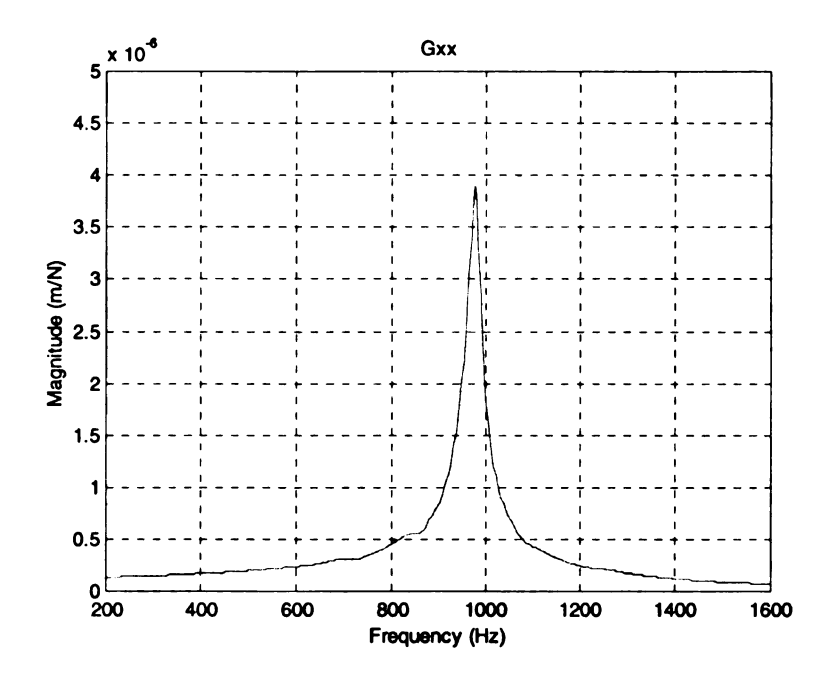


Fig. 10 Magnitude of transfer function $G_{xx}(s)$

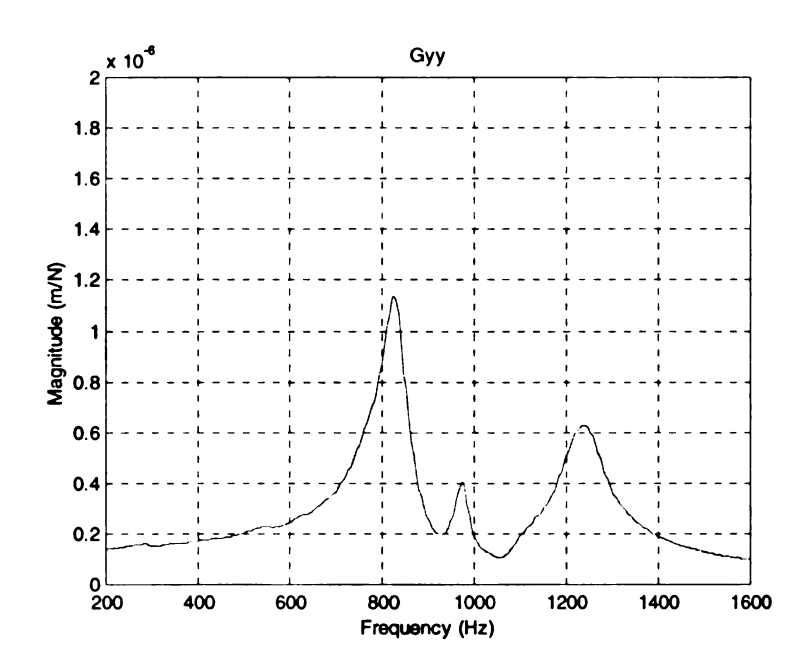


Fig. 11 Magnitude of transfer function $G_{yy}(s)$

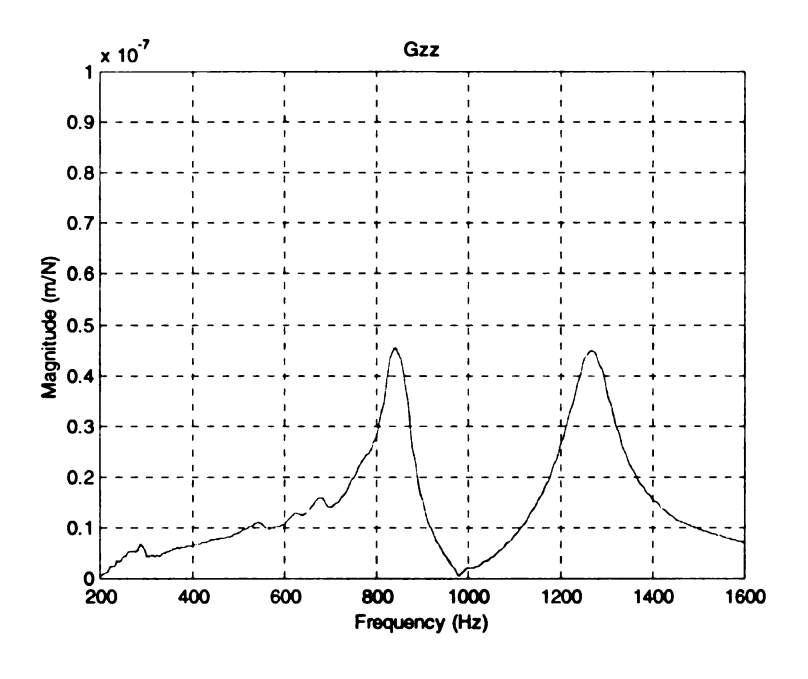


Fig.12 Magnitude of transfer function $G_{zz}(s)$

Table 3: Modal parameters of the Short bar

	ω _n (Hz)	K(N/m)	ξ
X	973.78	1.682e6	0.0769
Y	832.83	5.853e6	0.0760
Z	844.0	1.603e8	0.0688
Z	1264.5	5.596e8	0.0199

Two frequencies in the Z-direction were observed. Both the frequencies have been tabulated. The highest peak in the plot of transfer function $G_{xx}(s)$ has only been tabulated. The appearance of the other peaks is due to misalignment of the accelerometer in the X-direction which has therefore partially taken the responses of the Y and Z directions also.

Cutting tests were performed between the speed range of 900 and 4000 rpm. Stable cutting depths were used to compute the cutting coefficients. A plot of the axial accelerations recorded during a stable depth of cut operation of the short boring bar is shown in fig. 13. Fig. 14 shows the axial accelerations for an unstable depth of cut. The speed of revolution is 1980 rpm and the feed was 0.0141 mm/rev. Both the force plots were observed for a time scale of 5.7 seconds using a sampling interval of 50 μ s. Acceleration data recorded in the *X* and *Y* directions show a similar trend. However, their amplitudes were much different and lower than the amplitudes in the *Z* direction.

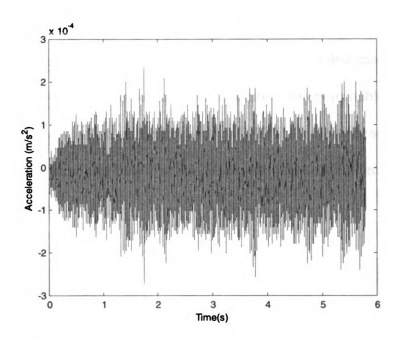


Fig.13 Axial accelerations for stable depth of cut 0.381 mm

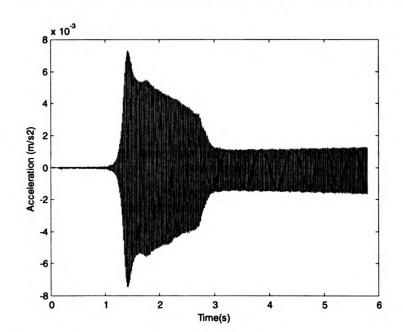


Fig.14 Axial accelerations for unstable depth of cut 1.016 mm

An FFT analysis was done for each second of the acceleration plots. The analysis showed a single frequency peak for the stable depth of cut. The peak frequency was 978

Hz, which is closest to the modal frequency in the x-direction. The frequency remained the same throughout the cutting operation. However, for the unstable case as shown by Fig. 14, the frequency builds up harmonics as the operation enters unstable depth of cut. The frequency also shifts from the stable frequency of 973 Hz to a frequency of 1297 Hz. Harmonics of 1297 Hz were also found in the acceleration plots. FFT analysis plots are shown in figs. 15 thru 18.

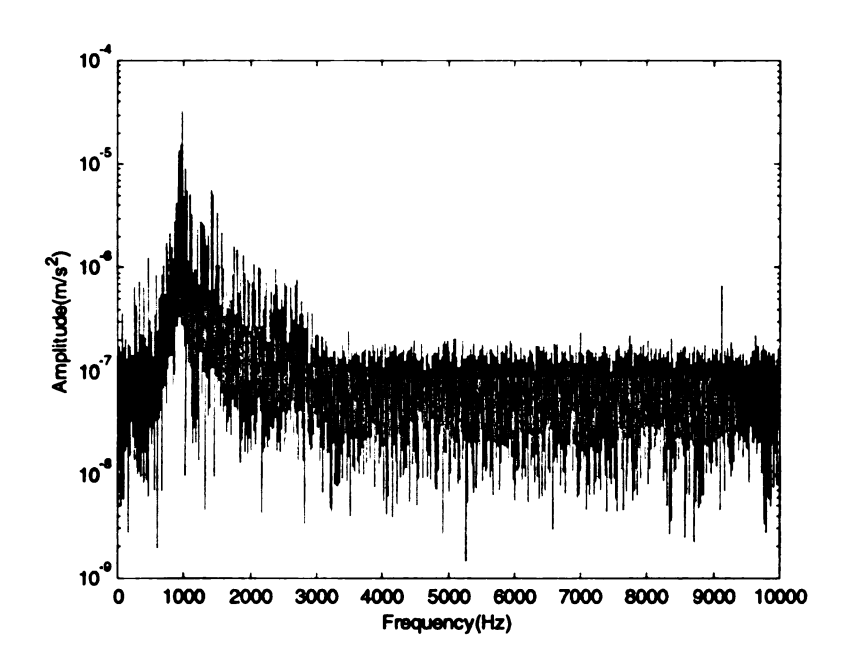


Fig. 15 FFT analysis for the 1st second of stable cut operation

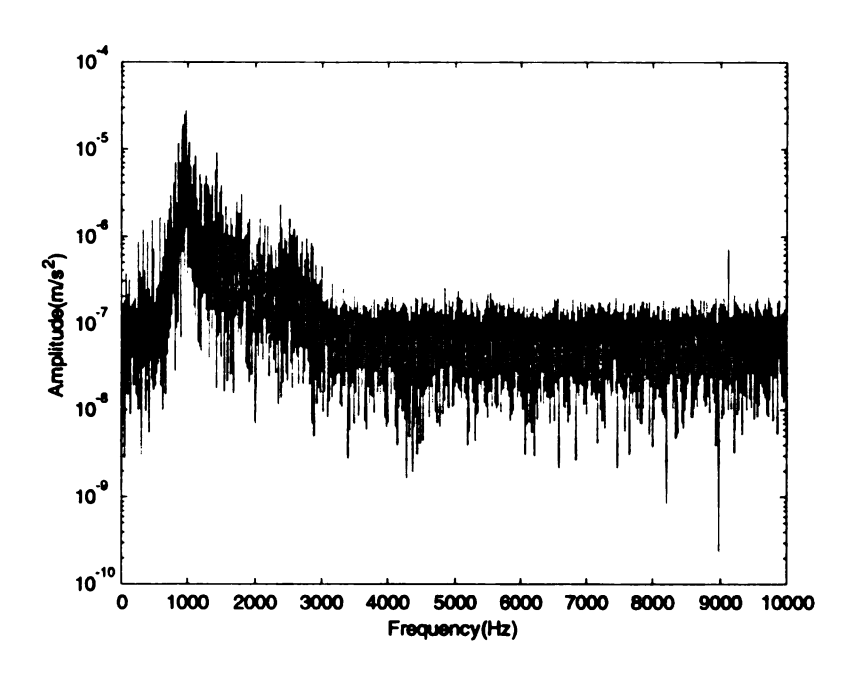


Fig. 16 FFT analysis for the 5th second of stable cut operation

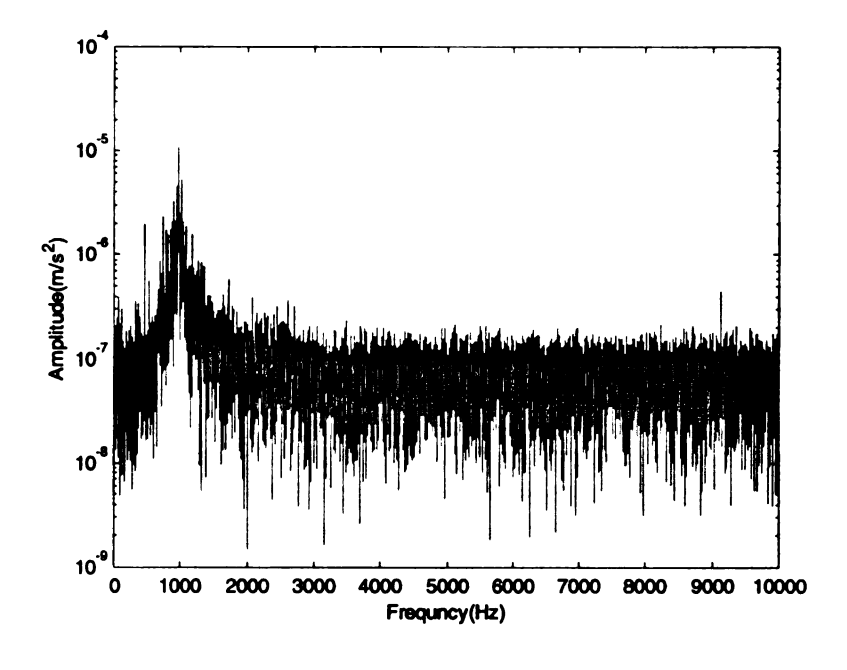


Fig. 17 FFT analysis for the 1st second of unstable cut operation

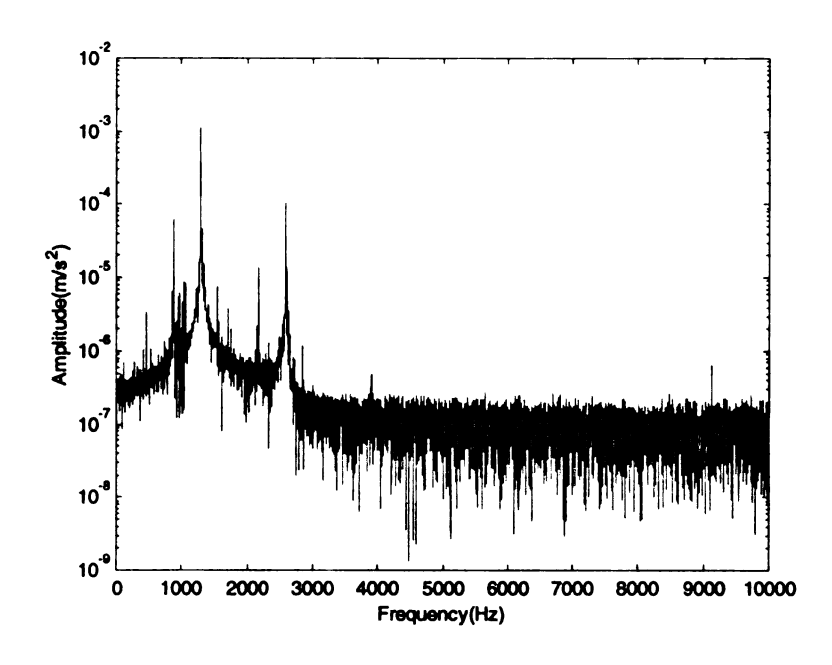


Fig. 18 FFT analysis for the 5th second of unstable cut operation

The properties given in Table 3 along with empirical cutting coefficients obtained from cutting processes between the tool and the workpiece (material AISI 10-45) were considered. Linearized cutting coefficients were used between speed ranges of 900 and 4050 rpm. Fig. 19 shows the stability lobes for the short boring bar between 2800 and 3600 rpm. The lobes were cross verified with experimental data obtained by performing cutting tests.

Table 4. Table of Cutting Coefficients

CUTTING COEFFICIENTS	N/MM^2
Radial (K _r)	8.29e8
Tangential (K _t)	1.9029e10
Axial (K _{ax})	9.5e9

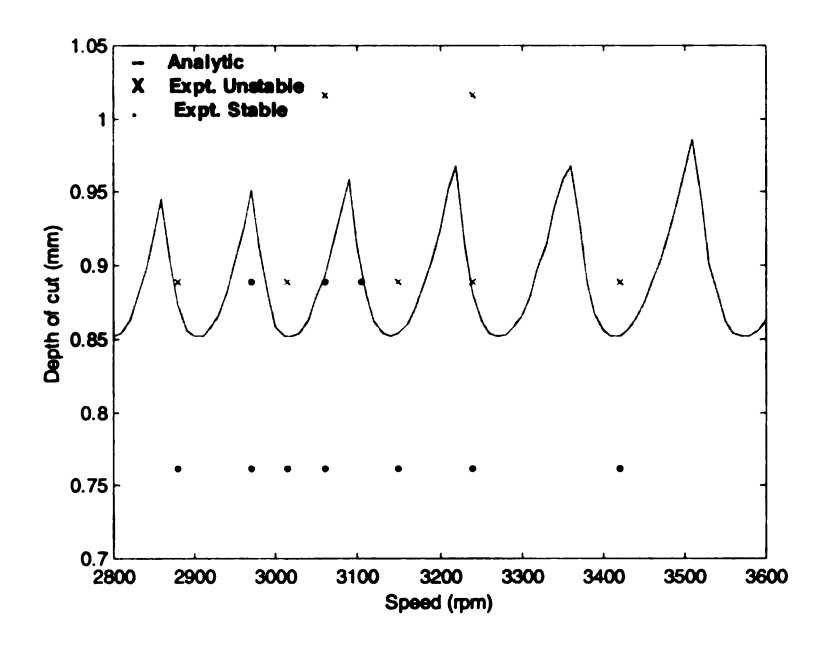


Fig. 19 Stability Lobes for the short boring bar

Experimental data was run in speed steps of 180 rpm. Around 3060 rpm, the speed steps were reduced to 90 rpm. Further, the operation was done at speeds of 3015 and 3105 rpm, a change of 45 rpm from the spindle speed of 3060 rpm. Depths of cut were run in steps of 0.005 inches starting from 0.03 inches. It can be observed from fig. 19 that the points observed through experiment were consistent with the analytic prediction. The experiment shows the existence of stable regions between the depths of cut of 0.75 and 1 mm.

Fig. 20 shows the chatter frequency simulated from the frequency domain analysis. The figure is obtained from the frequency domain analysis. Every point on the frequency domain stability lobe is attached to a chatter frequency ω Fig. 20 is a plot of the chatter frequency versus the spindle speed, again obtained from the time domain

analysis. Comparision of peak frequencies of the unstable region of cut shown by Fig. 18 shows that the chatter frequency plot in Fig. 20 is consistent with the experiment. Also, the chatter frequency was observed to be around 1300 Hz. The nearest modal frequency of the tool is the Z-axis frequency. It can be inferred that the presence of this high frequency in the tool results in the tool chattering near the range of 1300 Hz. Hence modal parameters in the Z-directions are important in a boring operation.

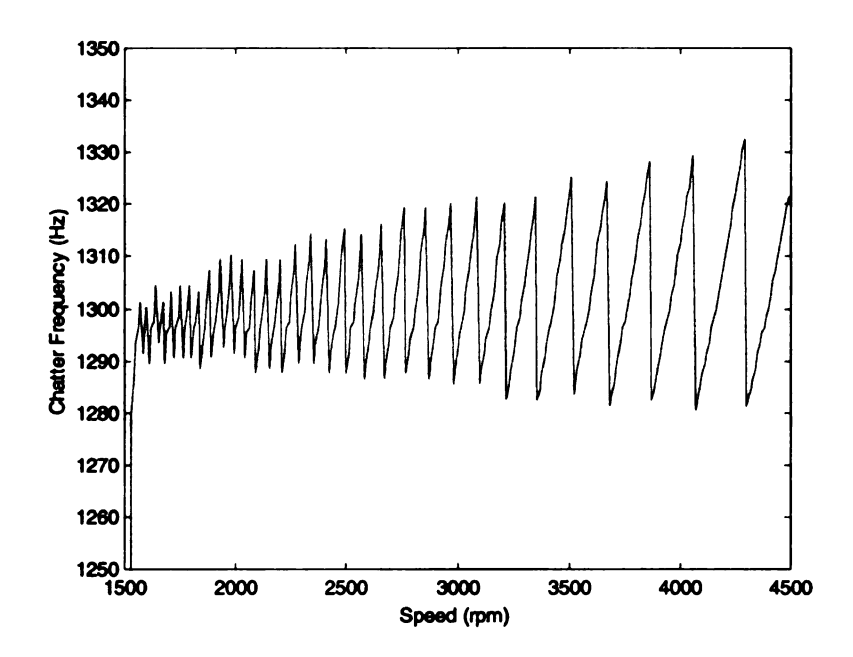


Fig. 20 Chatter signature of the short boring bar.

Section 4.2.2: Long Boring Bar (127 mm Overhang from the face holder)

In a second experiment a long boring bar of 127 mm overhang from the tool face holder was taken. The cutting setup was the same as the short boring bar. The insert used

was a Kennametal TNMA332 Carbide uncoated Insert. The workpiece used in the operation was steel of the quality AISI 10-45. The cutting coefficients were the same as used in the short boring operation before. The nose radius was eliminated by grinding the insert. The lead angle in the insert was 0°. Impact hammer tests revealed the following direct transfer functions and their respective modal parameters.

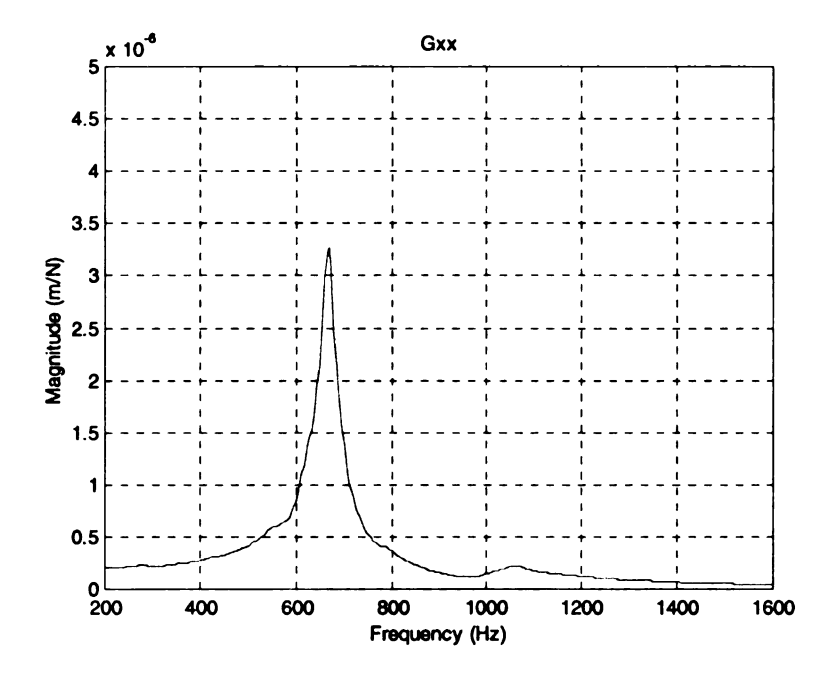


Fig. 21 Magnitude of Transfer function $G_{xx}(s)$

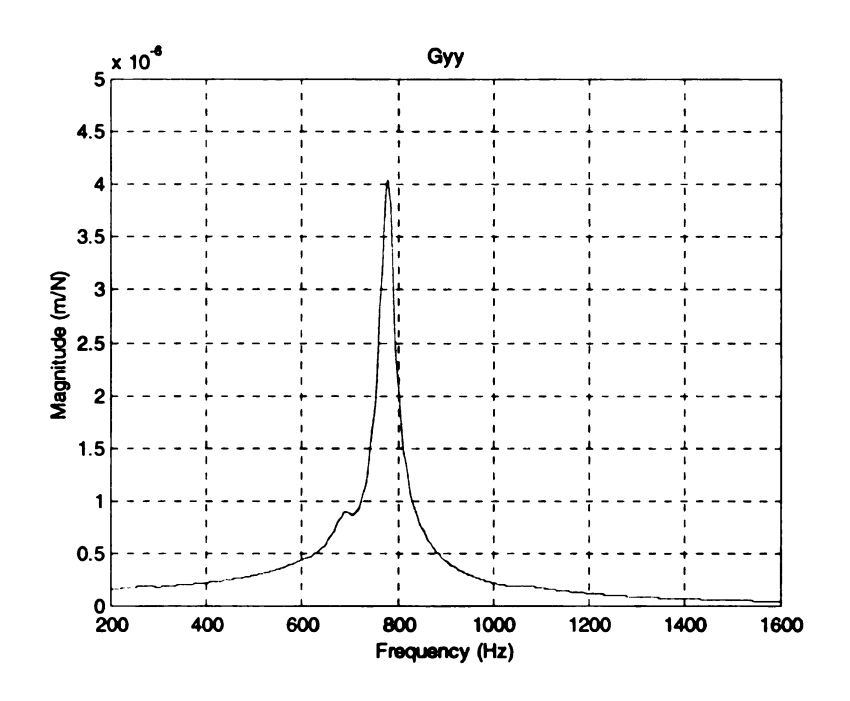


Fig. 22 Magnitude of Transfer function $G_{yy}(s)$

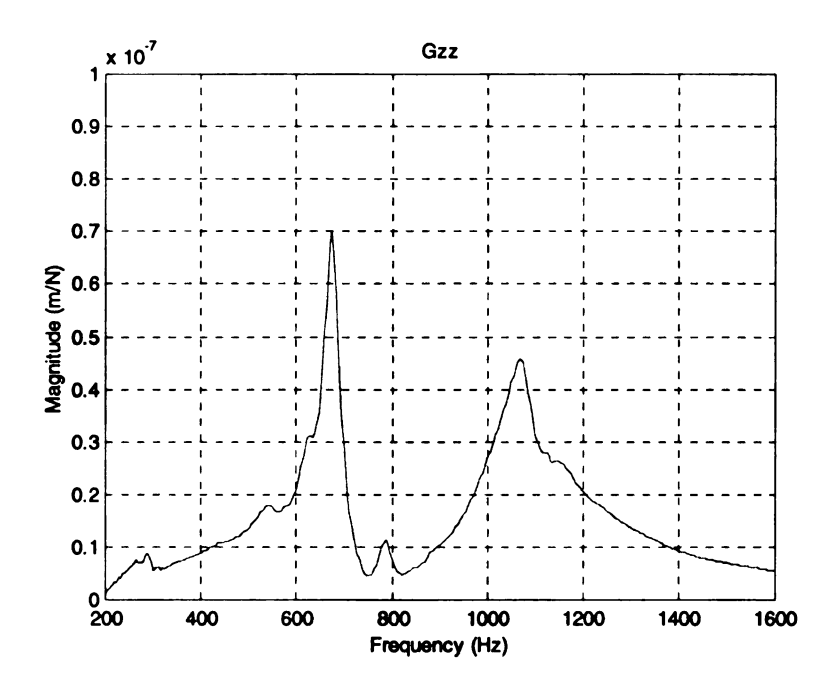


Fig. 23 Magnitude of Transfer function $G_{zz}(s)$

Table 5: Modal parameters of the Long bar

	ω _n (Hz)	K(N/m)	ξ
X	666.768	3.8462e6	0.0402
Y	777.155	5.5556e6	0.0227
Z	677.84	1.25e8	0.0589
Z	1066.5	4.375e8	0.0159

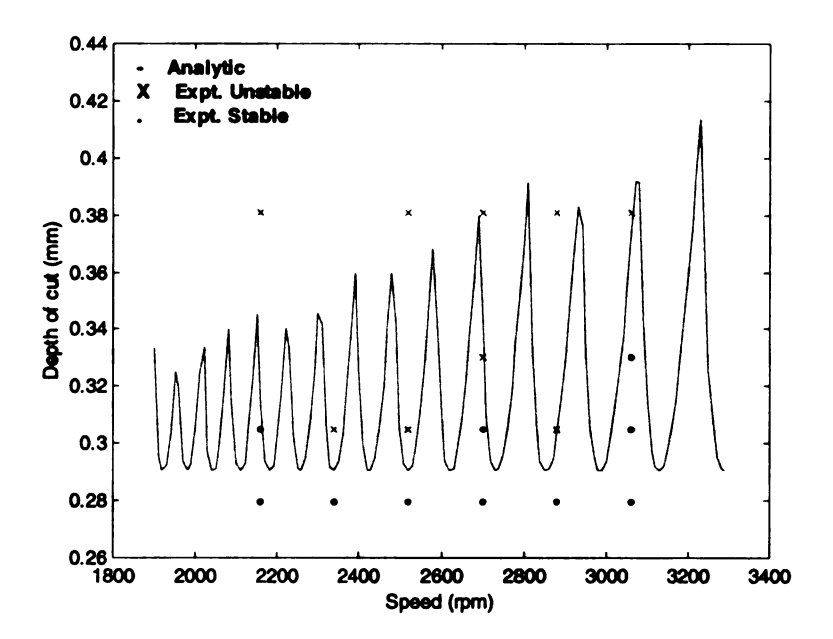


Fig. 24 Stability Lobes for the Long Boring Bar

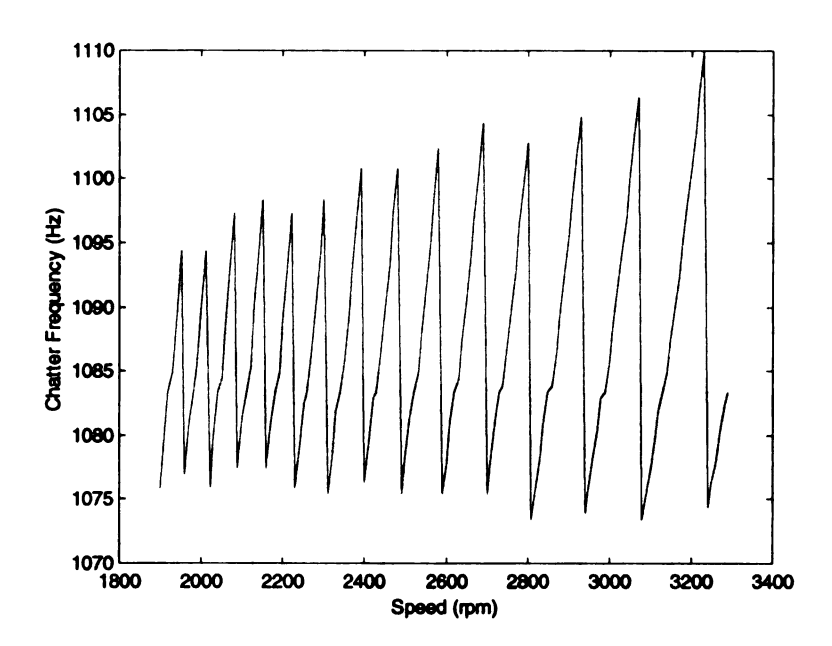


Fig. 25 Chatter Signature of the Long boring bar.

Fig. 22 shows the stability lobes for the long boring bar. The analytical simulation matched the experimental results well. Further resolution could not be achieved since the machine had a least depth of cut of 0.0254 mm. Observation of the chatter frequency in Fig. 25 showed the frequency to average around 1085 Hz, just above the second Z-axis modal frequency of the tool. FFT's of stable and unstable cuts are shown in Figs. 26 and 27.

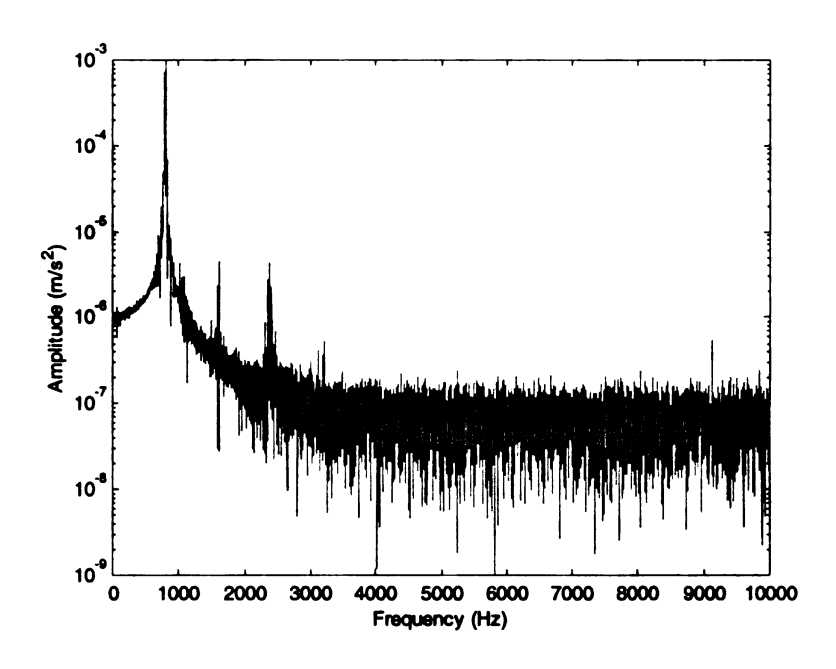


Fig. 26 FFT analysis for the 3rd second of a stable cut operation.

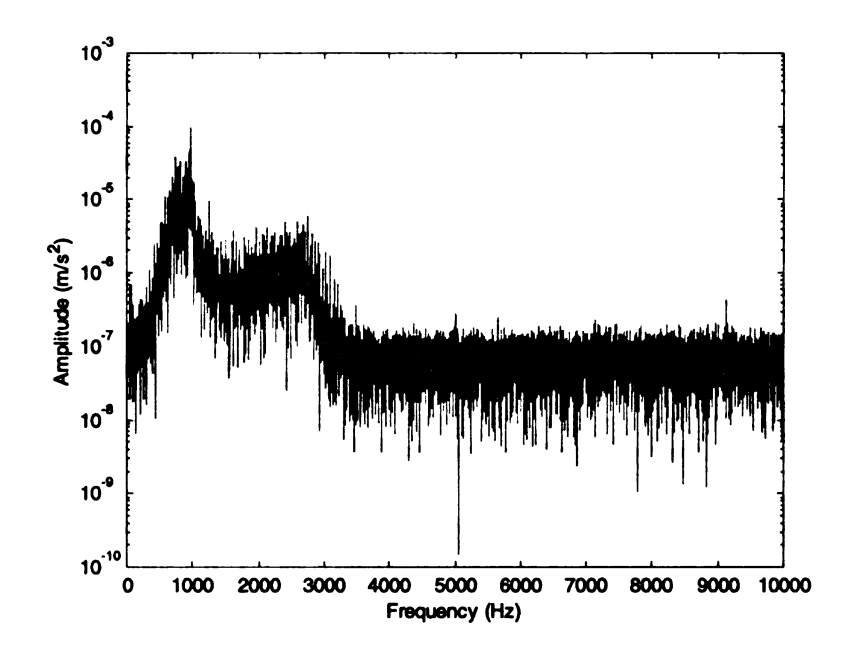


Fig. 27 FFT analysis for the 3rd second of an unstable cut operation

There exists a difference between the chatter frequency predicted and the FFT plot obtained for an unstable cut operaton. It can be observed from figure 27 that there

are more than one frequency that are active and important contrary to the prediction of a single chatter frequency for the long boring bar shown in figure 25. The discrepancy is possibily due to other non linear effects occurring during chatter on the long boring bar. The reasons for this discrepancy are under investigation. Detailed analysis for long boring bars has been left for future work.

Section 4.3: Discussion

The results from the experimental analysis show that the theory is well suited to deal with mid-speed range boring problems. The analytic prediction for a single insert operation as shown in Figs. 7 and 8 took 15 seconds to predict, whereas each point from the time domain simulation in the same figures took 15 seconds to generate. The complete time domain prediction therefore depends strongly upon the number of cases that were run and the number of revolutions simulated, which is very time consuming.

In Eq. 7, to calculate the chip area, the static chip area has been removed because it doesn't cause any regeneration. The dynamic chip area has a first order approximation that is used for frequency analysis. The analytic prediction as seen from the Figs. 7 and 8 show that the approximation made is valid.

Another approximation made in this theory is that the cutting coefficients are constant. In actual practice, cutting coefficients are functions of speed and depth of cut [27]. However, cutting forces vary a lot in the low speed range machining processes.

Cutting forces are fairly constant in the mid range and higher range speed machining forces.

The lead angle is observed to play a crucial role in the analysis. Typically boring bars have lead angles varying from -20° to +20° [31]. Lead angles away from 0° result in more influence of the transverse transfer functions, Gxx and Gyy in the solution. The primary influence on the solution is from the axial direction. Hence the modal parameters in the axial direction, though stiffer than the transverse direction, are important in the analysis. This is shown by the experimental observation of chatter frequency from Fig. 18. The frequency at which the system shown instability is close to 1300 Hz, which is near the modal frequency in the Z-direction of the boring bar.

The nose radius of a tool is another parameter which has not been considered here. Nose radius typically exists for curved tools. This analysis has been performed for tools without a nose radius. The formulation can be easily changed to accommodate the influence of nose radius. Experiments performed with the short boring bar showed unstable cutting at very low depths of cut. This is attributed to the fact that in the presence of the nose radius, cutting at very low depths of cut changes the angle of contact between the insert and the workpiece, thereby changing the cutting force angles. This was most probably the case of observation of chatter at very low depths of cut. The nose radius was practically eliminated in the long boring bar insert. In practice, it is not advisable to work without a nose radius because it tends to cause excessive stress concentrations at the tip. However, it is possible to work at depths of cut much higher

than the nose radius, as was shown by the experiments with the short boring bar.

The regeneration factor has also been taken as 1, similar to earlier approximations done before for mid range and high speed range boring process [27]. For very low speed processes, this will not be valid as the ratio of feed rate to the speed of operation becomes large.

Cutting coefficients earlier used were radial velocity, radial displacement, axial displacement and tangential displacement coefficients [25]. These coefficients have been done with and simpler coefficients, i.e., tangential, radial and axial have been incorporated, all dependant on the dynamic chip area.

Aspects such as friction have been disregarded. Friction forces gain importance only at very low low speed range of machining, where it is possible that the machine tool just rubs the surface of the workpiece without actually cutting it. Industry demands processes to be high speed so that material removal rates are high, therefore increasing productivity.

Chapter 5: Conclusions

- A new analytical theory has been developed to predict the stability limits for boring in mid speed and high speed range operations. The theory assumes regeneration to occur in the axial direction of the boring bar.
- 2. Results of the theory agree with those of the time domain simulation.
- 3. The time taken for generation of stability lobes is very small as compared to the time for generating the lobes using a classical time domain simulation. Hence, the analytic method is a quick tool to generate stability lobes for a boring operation.
- 4. The regenerative forces are assumed proportional to the dynamic chip area, thereby making the analysis simpler.
- 5. The observed and predicted chatter frequencies for a short boring bar agree with each other.
- Friction and tool rubbing aspects have been excluded since the range of operation is mid speed and high speed.
- 7. This theory is presently employed at the industry.

Chapter 6: Suggestions for future work

The cutting coefficients used in this work are linearized, much like those in earlier work [14, 18, 19]. An indepth study of the coefficients for the range of speeds of the operation has been left for future work. The cutting coefficients may exhibit non-linear behaviour at low speeds, and so the analysis has to be modified including the non-linear effects of the cutting coefficients at lower speeds. Cutting coefficients could possibly be obtained by non-linear techniques such as parameter estimation and harmonic balancing.

Existence of friction and tool rubbing without cutting have been observed. This analytic model assumes that the machine tool cuts the workpiece everytime it is in contact with it. Friction and tool rubbing normally occur at low speeds of machining, where the surface speed becomes very low. New models could be developed incorporating these aspects.

As seen from the results, the chatter frequencies matched well for the short boring bar and not for the long one. Current work at Boeing investigates the possible existence of chatter frequencies below the modal frequencies of the tool for a drilling process. It is quite possible that the analysis presented in this work could be extended in that direction, to suitably predict the chatter frequencies.

Bibliography

- Merchant, M.E., Mechanics of the metal cutting process, J. Appl. Phys., 16, 267,
 1945.
- 2. Astakhov, Viktor P., Metal Cutting Mechanics, 1998.
- 3. DeVries, Warren R., Analysis of Material Removal Processes, 1992
- Merritt, H.E., "Theory of Self-Excited Machine Tool Chatter- Contribution to Machine Tool Chatter Research-1," Journal of Engg. For Industry, Trans. ASME, Series B, Vol.87, No.4, Nov.1965, pp.447-454.
- 5. Smith S., and Tlusty J., "Current trends in High speed Machining," Transactions of the ASME, Vol. 119, November 1997, pp. 664-666.
- 6. Smith, S., and Tlusty J., "Update on high speed milling dynamics," Transactions of the ASME, Vol. 112, May 1990, pp. 142-149.
- 7. Tlusty J., Zaton, W. "Stability lobes in milling," Annals of the CIRP Vol.32/1/1983, pp.309-313.
- 8. Fishwick W., Tobias S.A., "Machine Tool Chatter, Effect of Flexibility in Machine and Foundation," Engineering, 1958, pp. 568-572.
- 9. Sridhar et. al., "A general formulation of the milling process equation, Contribution to Machine Tool Chatter Research-5," J. Engg. Industry, 1968, pp. 317-324.
- 10. Sridhar et. al., "A stability algorithm for the general milling process, Contribution to Machine Tool Chatter Research-7," J. Engg. Industry, 1968, pp. 330-334.

- 11. Smith S., Tlusty J., "Stabilizing Chatter by Automatic Spindle Speed Regulation,"
 Annals of the CIRP Vol.41/1/1992, pp. 433-436.
- 12. Smith S., Tlusty J., "Efficient Simulation Programs for Chatter in Milling,"
 Annals of the CIRP Vol.42/1/1993, pp. 463-466.
- 13. Minis I., Yanushevsky R., "A new theoretical approach fot the prediction of Machine Tool Chater in milling," J. Engg. Industry 1993, Vol 115., pp.1-8.
- 14. Altintas Y., Budak E., "Analytical Prediction of Stability Lobes in Milling,"
 Annals of the CIRP Vol.44/1/1995, pp. 357-362.
- 15. Thusty J., 1996, "Techniques for the Use of Long Slender End Mills in High Speed Milling," Annals of the CIRP Vol. 45/1/96.
- 16. Chen S.-G., Ulsoy A.G., Koren Y., "Computational Stability of Chatter in Turning," ASME J. Manuf. Sc. Engg., November 1997, Vol. 119, pp.457-460.
- 17. Rao B.C, Shin Y.C., "A comprehensive dynamic cutting force model for chatter prediction in turning," Intl. J. Machine Tools & Manuf., 39 (1999) 1631-1654.
- 18. Bayly P.V., Halley J.E., Young K.A, "Tool Oscillation and the formation of Lobed Holes in a Quasi-static model of Reaming," ASME DETC99/VIB-8061
- 19. Bayly P.V., Halley J.E., Young K.A, Metzler S.A., "Analysis and simulation of Radial Chatter in Drilling and Reaming," ASME DETC99/VIB-8059
- Ansoff, H.I. "Stability of linear oscillating systems with constant time lag," J.
 Appl. Mech., Trans. Am. Soc. Mech. Engrs. 1949 16, 158.
- 21. Tlusty, J. "Berechnung des Rahmens der Werkzeug-maschinen," Schwerindustrie der Tschechoslovakei 1955 (No.1), 8.

- 22. Parker, E.W., 1970, "Dynamic Stability of a Cantilever Boring Bar with Machined Flats under Regenerative Cutting Conditions," J. Mech. Engr. Sc., Vol. 12, No.2, pp.104-115.
- 23. Rivin, E.I., 1983, "A Chatter-Resistant Cantilever Boring Bar," Proceedings of North American Manufacturing Research Conference, Society of Manufacturing Engineers, Dearborn, MI.
- 24. Kapoor, S.G., Zhang, G.M., Bahney, L.L., 1984, "Stability Analysis of the Boring Process System," Proceedings of North American Manufacturing Research Conference, SME, Dearborn, MI.
- 25. Zhang, G.M., and Kapoor, S.G., 1987, "Dynamic Modeling and Analysis of the boring Machining System," ASME Journal of Engineering for Industry, Vol. 109, pp.219-226.
- 26. Tewani, S.G., Rouch, K.E., Walcott, B.L., 1993, "A study of Cutting Process Stability of a Boring Bar with Active Dynamic Absorber," Int. J. Mach. Tools Manufact., Vol.35, No.1, pp.91-108, 1995.
- 27. Li, C-J., Ulsoy, A.G., Endres, W.J., "The effect of Tool Rotation on Regenerative Chatter in Line Boring," in R.P.S. Han, K.H. Lee and A.C.J. Luo, Eds., Dynamics, Acoustics and Simulations, ASME Publication DE-Vol.98, pp.235-243, 1998.
- Ozdoganlar, O.B., Endres, W.J., "An Analytical, non-dimensional representation of chip-area for corner radiused tools under depth-of-cut and feed variations," MED-Vol.8, Proceedings of the ASME Manufacturing Science and Engineering Division, 1998.

- 29. Landers, R.G., Ulsoy A.G., "Chatter Analysis of Machining Systems with nonlinear force processes," DSC_Vol.58, Proceedings of the ASME Dynamics Systems and Control Division, ASME 1996.
- 30. Rao, B., and Shin, Y. C., (1999), "A Comprehensive Dynamic Cutting Force Model for Chatter Prediction in Turning," *International Journal of Machine Tools and Manufacture*, Vol. 39, pp. 1631-1654.
- 31. Kennametal Manual for Metalcutting Tools, Kennametal Inc., Latrobe, Pennsylvania.
- Jayaram, S., (1997), "Stability and Vibration Analysis of Turning and Face Milling Processes," Ph. D. Thesis, University of Illinois at U-C.
- 33. Driver, R.D., (1976), "Ordinary & Delay Differential Equations," Applied Mathematical Sciences 20.
- 34. Meinardus, G. and Nurnberger, G. eds., "Delay Equations, Approximations and Applications," [1985], International Symposium at the University of Mannheim, Oct8-11, 1984.
- 35. Shaw, M. C., "Metal Cutting Principles," Clarendon Press, Oxford, 1984.

Appendix A

